Dully, M., Brasnett, C., Djeghader, A., Seddon, A., Neilan, J., Murray, D., Butler, J., Soulimane, T., & Hudson, S. P. (2020). Modulating the release of pharmaceuticals from lipid cubic phases using a lipase inhibitor. *Journal of Colloid and Interface Science*, *573*, 176-192. https://doi.org/10.1016/j.jcis.2020.04.015

Journal of Colloid and Interface Science 573 (2020) 176–192

Contents lists available at ScienceDirect

Journal of Colloid and Interface Science

journal homepage: www.elsevier.com/locate/jcis

# Modulating the release of pharmaceuticals from lipid cubic phases using a lipase inhibitor

Michele Dully [a], Christopher Brasnett [b], Ahmed Djeghader [a], Annela Seddon [b,c], John Neilan [d], David Murray [d], James Butler [d], Tewfik Soulimane [a,*], Sarah P. Hudson [a,*]

[a] Department of Chemical Sciences, Bernal Institute, University of Limerick, Castletroy, Co. Limerick, Ireland
[b] School of Physics, University of Bristol, Tyndall Ave, Bristol BS8 1FD, United Kingdom
[c] Bristol Centre for Functional Nanomaterials, HH Wills Physics Laboratory, Tyndall Avenue, University of Bristol, Bristol BS8 1FD, United Kingdom
[d] COOK Ireland Limited, O'Halloran Rd, Castletroy, Co. Limerick, Ireland

## GRAPHICAL ABSTRACT

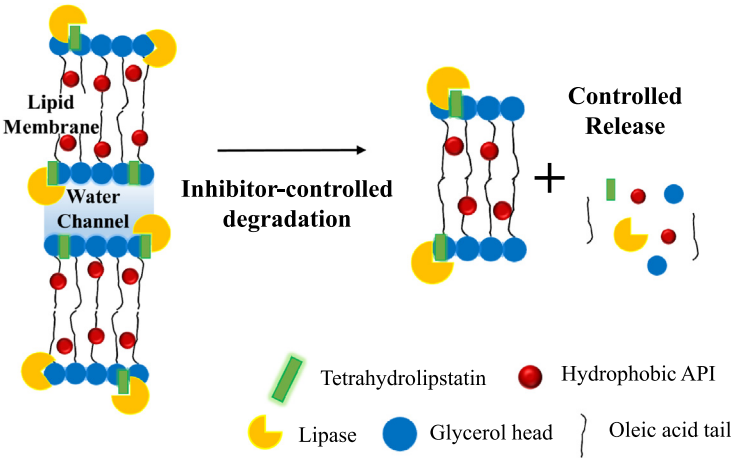


## ARTICLE INFO

*Article history:*
Received 10 February 2020
Revised 2 April 2020
Accepted 3 April 2020
Available online 4 April 2020

*Keywords:*
Lipid cubic phase
Controlled delivery
Hydrophobic active pharmaceuticals
Enzyme degradation
Lipase inhibitor
SAXS

## ABSTRACT

Lipid cubic phase formulations have gained recognition as potential controlled delivery systems for a range of active pharmaceutical and biological agents on account of their desirable physiochemical properties and ability to encapsulate both hydrophobic and hydrophilic molecules. The most widely studied lipid cubic systems are those of the monoacylglycerol lipid family. These formulations are susceptible to lipolysis by a variety of enzymes, including lipases and esterases, which attack the ester bond present on the lipid chain bridging the oleic acid component to the glycerol backbone. The release of poorly soluble molecules residing in the lipid membrane portions of the phase is limited by the breakdown of the matrix; thus, presenting a potential means for further controlling and sustaining the release of therapeutic agents by targeting the matrix stability and its rate of degradation. The aims of the present study were twofold: to evaluate an approach to regulate the rate of degradation of lipid cubic phase drug delivery systems by targeting the enzyme interactions responsible for their demise; and to study the subsequent drug release profiles from bulk lipid cubic gels using model drugs of contrasting hydrophobicity. Here, hybrid materials consisting of cubic phases with monoacylglycerol lipids of different chain lengths formulated with a potent lipase inhibitor tetrahydrolipstatin were designed. Modulation of the release of

* Corresponding authors at: Bernal Institute, University of Limerick, Castletroy, Limerick, Ireland.
*E-mail addresses:* tewfik.soulimane@ul.ie (T. Soulimane), sarah.hudson@ul.ie (S.P. Hudson).

https://doi.org/10.1016/j.jcis.2020.04.015
0021-9797/

a hydrophobic model pharmaceutical, a clofazimine salt, was obtained by exploiting the matrices' enzyme-driven digestion. A stable cubic phase is described, displaying controlled degradation with at least a 4-fold improvement compared to the blank systems shown in inhibitor-containing cubic systems. Sustained release of the model hydrophobic pharmaceutical was studied over 30 days to highlight the advantage of incorporating an inhibitor into the cubic network to achieve tunable lipid release systems. This is done without negatively affecting the structure of the matrix itself, as shown by comprehensive small-angle x-ray scattering experiments.


## 1. Introduction

Challenges in the delivery of therapeutic agents *in vivo* include controlling and maintaining their release at therapeutically effective doses over a sustained period of time, long enough for them to exhibit their desired effect. Smart design of delivery systems can help overcome these challenges. This is particularly applicable in the design of delivery matrices for pharmaceuticals of poor water solubility, which is believed to account for between 70 and 90% of new drugs in development [1,2]. Lipid carrier systems have proven their potential in controlled delivery applications on account of their unique microstructure and amphiphilic character, as well as the biodegradable and biocompatible nature of the lipids used [3,4]. Lipids, in different forms, have been widely utilized [5–7]; from liposomes to lipid-derived nanoparticles [8,9] and both as solid-state [10], and dispersed matrices [11,12].

One particular system, the lipid cubic phase, has generated interest as a sustained delivery vehicle over the past two decades [13]. These systems possess a unique microstructure [14–17] that can be accessed under certain conditions of temperature and water content [4,18], and have demonstrated their capacity to encapsulate and control the delivery of a wide range of pharmaceuticals of different solubilities from enzymes and proteins to small molecule drugs. Additionally, their inherent thermostability, even in excess water, make the cubic phase and its dispersions attractive vehicles for *in vivo* applications [19,20]. Lipid cubic phase formulations have been used as transporters of both small molecules and larger proteins through both oral [21,22] and parenteral routes as well as in local delivery applications including subcutaneous and intramuscular routes [13,23–25]. They have been utilized as sustained release systems for a range of pharmaceutical agents of different aqueous solubilities [26–30], the majority of which demonstrate diffusion-controlled release that follows first order kinetics. Numerous commercially available host lipids [3,14,28,31–33] capable of forming the cubic phase exist and the selection of a suitable host is key in developing the cubic phase for drug delivery applications.

The matrix's application in sustained release, while proven to be very promising, is somewhat limited as a consequence of its shorter release profile which is often less than 24 h for hydrophilic agents [13,28] and its highly viscous consistency which has been likened to toothpaste [34]. Additionally, the integrity of monoacylglycerol derived cubic phase (MAG LCPs) gels in particular are greatly compromised by the presence of lipolytic enzymes [28,35,36] – likely influencing the release kinetics of any membrane-embedded hydrophobic drugs with which it is formulated as has been described for numerous hydrogel systems [37]. These MAG lipid systems are subject to slow hydrolysis at the ester linkage connecting the acyl chain (oleic acid) to the glycerol backbone [35,36,38]. The main perpetrators are a family of enzymes, lipases, that are found in the body, often accompanied by other offending abettors such as esterases. Lipases are water-soluble and act at an oil-water interface during lipolysis of triglycerides in any aqueous system through a series of intricate steps [35], with the surface area being the rate limiting factor [36,39].

The inhibition of lipase interactions through steric approaches has previously been described as a means to impede the digestion of lipid-based formulations for drug delivery [40–44]. Additionally, a class of lipids exist that have been synthesized such that their structure greatly resembles that of monoolein, except that the glyceryl ester group is replaced by a glycerate [45]. As an alternative, here we present a novel chemical approach to achieve regulated degradation and subsequent controlled drug release from bulk lipid cubic systems by targeting these lipase enzyme interactions through the incorporation of a known inhibitor into the lipid network. The stability of two bulk LCP matrices is examined over time in the presence of a hydrophilic or a hydrophobic active pharmaceutical ingredient (API) and in the presence of tetrahydrolipstatin (THL), a potent active site-directed lipase inhibitor [46–50]. THL is FDA approved and indicated for the treatment of obesity at concentrations that well exceed those used in this study [51]. A surface loop system employed by pancreatic lipases controls access to their active site. In the presence of lipid substrates and other amphiphiles, the surface loop, or 'lid', undergoes a conformational change thus exposing the enzyme's catalytic site [52]. Upon exposure, tetrahydrolipstatin exerts its inhibitory effect upon binding the pancreatic lipase at its catalytic serine residue as it forms a stable monolayer at the oil-water interface [42,53,54]. Following a nucleophilic attack of the serine active site on the b-lactone group [55,56], the THL forms a stoichiometric acyl-enzyme complex with the various lipases [46,47,57] to impede the catalytic degradation of the lipid formulation (Schematic displayed in the supplementary information).

Lipolysis and its inhibition are considered to be a set of competitive processes, often occurring simultaneously both *in vitro* and in biological systems when an inhibitor and a lipid substrate co-exist [58]. The efficacy and rate of the individual processes are dependent on factors including concentration and surface area and are related to the ratio of lipid substrate to enzyme inhibitor. The inhibitor selected in this investigation was incorporated into the lipid cubic gels at different concentrations in a bid to stabilize and control their digestion by pancreatic lipase. A range of THL loadings from 0.35 to 2.5 wt% were selected to demonstrate the relationship between inhibitor concentration and the rate of competitive lipolysis, subsequently allowing for the tunable degradation-driven release of hydrophobic pharmaceuticals from their network. Within this range of inhibitor concentrations, the cubic phase is accessed and maintained under the experimental conditions described in this investigation, without any observed phase transition.

THL is practically insoluble in water [59] and so was expected to reside mainly in the lipidic domain of the cubic phase, while its hydrophilic portions may partition into the aqueous channel compartment. In a similar way that a lipid/water interface is necessary for lipase catalysis, inhibition of the enzyme by THL is possible at this boundary [39,53]. This means that most likely only the THL available at the surface of the lipid network in the LCP can carry out its inhibitory function while the THL integrated in the inner bilayers would serve as a reservoir, reaching the lipid/water interface upon the degradation of the gel [40,60,61]. This repository provides fresh inhibitor to the system for the entirety of its life,

where continuous, controlled degradation at the surface of the gel exposes encapsulated THL to the lipolytic enzyme. A clofazimine citrate salt and caffeine were selected as model APIs for release studies based on their different propensities to dissolve in water (~40 mg/L [62] and ~51 g/L [63] at 37 °C for the CFZ-citrate and caffeine respectively). Their structures are shown in Fig. 1.

## 2. Material and methods

### 2.1. Materials

All solvents were analytical grade and purchased from FisherScientific; Monoolein 9.9 MAG (1-(9Z-octadecenoyl)-*rac*-glycerol) and Monopalmitolein 9.7 MAG (1-(9Z-hexadecenoyl)-*rac*-glycerol) were acquired from JenaBioscience, Germany at > 99% purity; Phosphate buffered saline (PBS) tablets were purchased from Merk (Saint Louis, MO); Water was purified in the lab using a Milli-Q Water System (Millipore Corporation, Bedford, MA); Clofazimine (CAS registry number 2030-63-9) was purchased from Beijing Mesochem Technology Co., Ltd. The clofazimine-citrate salt form was produced previously by our group [62]; Lipase isolated from porcine pancreas was purchased from Merck, Germany (Type II, 100–500 units/mg protein (using olive oil (30 min incubation)), 30–90 units/mg protein (using triacetin), L3126 SIGMA); Caffeine (99% purity, Sigma-Aldrich); Tetrahydrolipstatin (Orlistat) (99% purity, Sigma-Aldrich).

### 2.2. Preparation of MAG LCP matrix formulations

Viscous lipid cubic phase formulations were obtained by dispensing appropriate volumes of molten monoacylglycerol (MAG)

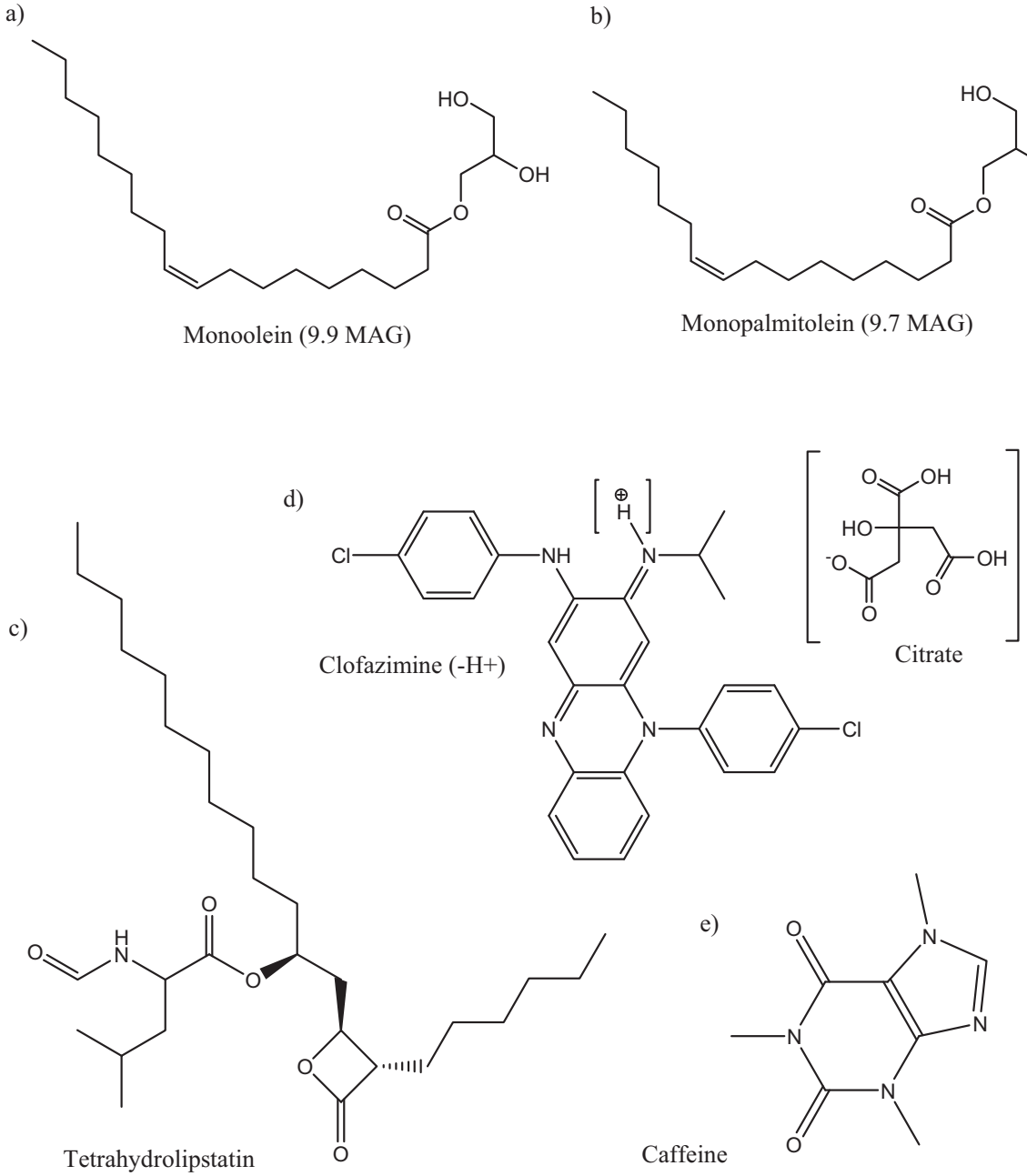


**Fig. 1.** Chemical structures of: (a) monoolein (9.9 MAG) and (b) monopalmitolein (9.7 MAG) both possessing an ester linkage linking the oleic acid chain to the glycerol backbone; (c) lipase inhibitor tetrahydrolipstatin (THL); (d) hydrophobic model active pharmaceutical ingredient (API) clofazimine-citrate; (e) hydrophilic model API caffeine.

(Monoolein (MO) ≥ 60 mg/sample or Monopalmitolein (MPL) ≥ 50 mg/sample) in glass vials. Fusion of dry MAG crystals to the melt was achieved at 40 °C. This was followed by the addition of the aqueous solution in excess volumes (≥45 wt% and ≥ 55 wt% for MO and MPL LCP respectively) according to their respective phase diagrams [18,32,64]. The samples were then subjected to vortex mixing for at least 15 min and equilibrated and stored in sealed glass vials out of direct light at room temperature until an optically clear and visually homogenous sample was achieved and for no longer than three weeks.

A range of MAG lipidic mixtures with 0.35, 0.7, 1.5 and 2.5 wt% THL were prepared by first dissolving the inhibitor in the appropriate weighed amounts of molten lipids. Homogeneous blends were achieved by subjecting the molten solution to brief vortex mixing with gentle heating. Mesophase samples were then generated by mixing weighed quantities of MAG lipid-THL formulations with Milli-Q water corresponding to ratios at excess hydration according to the MAG lipid-water phase diagrams (≥40% − 50% w/w).

The same approach was taken for the incorporation of the hydrophobic API (CFZ-citrate salt) into the LCP whereby the API crystals were dispersed in the molten MAG at the desired percentage weight before the introduction of water to the system to form the cubic phase. For the hydrophilic API, caffeine, the caffeine was dissolved in the water used to prepare the cubic phase and this was added to the blank molten lipid. Both the caffeine and the CFZ-citrate salt samples were prepared at concentrations of 1 and 3 wt% API.

### 2.3. Evaluation of MAG matrices

#### 2.3.1. Polarizing light microscopy

Polarized light was utilized to assign the predicted liquid crystalline mesophase accessed. A spatula tip of the generated mesophase was transferred to a glass microscope slide and immediately covered with a glass coverslip. The sample was examined under normal and cross polarized light at room temperature on a Zeiss AxioScope Optical microscope equipped with polarized light filter and a cross-polarizer. Image acquisition was carried out using an AxioVision 4.8 imaging system by Carl Zeiss Ltd. Non-birefringence in refraction was identified by the appearance of a black image or zone on the camera.

### 2.4. SAXS

Small angle X-ray scattering was performed to confirm mesophase assignments for the formulations and to assign lattice parameters.

#### 2.4.1. SAXS sample preparation

Mesophase samples with discrete composition were prepared as previously described for various concentrations of tetrahydrolipstatin within the range of 0 to 2.5 wt%. To study the metastability of the phases over a prolonged period of time, samples were prepared 3 weeks, 4 days, 2 days and 1 h prior to SAXS data collection. Samples were stored in sealed vials until just before data acquisition to avoid any sample dehydration through atmospheric exposure. Another set of samples were tested to determine the loading capabilities of the phase with the model APIs, prepared as previously described at concentrations of 1 and 3 wt%.

#### 2.4.2. SAXS data collection

SAXS measurements were carried out after sample preparation at the Solution State SAXS B21 beam line at Diamond Light Source on the Harwell Campus, Didcot, UK. The experiments used a beam of wavelength λ = 13.1 keV (~0.94644 Å) with a beam size at the sample of 1 mm × 1 mm. Data collection was performed at ambient temperature (20 °C). B21 utilizes a bending magnet source with a typical flux of approximately $4 \times 10^{12}$ photons per second delivered directly to the sample. The photons were distributed over a large 0.8 × 2 mm cross-section which served to minimize radiation damage while also enhancing the signal of the particles. 2D diffraction images were recorded on an Eiger X 4 M detector, with a detector face size of 155.2 mm × 162.5 mm and pixel size of 75 μm × 75 μm. The beam size at the detector was 50 μm × 50 μm. The detector was configured to measure a scattering vector (q) range from 0.0032 to 0.38 $Å^{-1}$. Samples were loaded into a custom 3-D printed sample holder designed especially for viscous samples. The holder was 3-D printed from a mixture of methacrylic acid esters and photoinitiator comprising a window in which the sample was filled. The sample holder was made from stainless steel and had mica windows. Each sample was subjected to a 1 s X-ray exposure for 15 frames at one location and required manual loading.

#### 2.4.3. SAXS data processing and analysis

Exposure of the lipid samples to the X-ray beam produced small angle diffraction images. The detector images were azimuthally reduced using DAWN, an eclipse-based workbench for carrying out scientific data analysis [65] and subsequently analysed using the lipidsaxs toolkit developed by Christopher Brasnett, University of Bristol, available at https://github.com//csbrasnett/lipidsaxs. The scattering intensity I (q) was represented as a function of the magnitude of the scattering vector $q = \frac{4\pi sin\theta}{\lambda}$ where 2θ is the total scattering angle.

### 2.5. Lipid cubic phase structural dimensions calculation

Taking into account the space group, lattice parameter and water volume fraction of each of the different samples, the monolayer thickness and size of the water channels separating the lipid framework was determined as outlined by Szlezak, Nieciecka [66] and according to the following equations:

To compute the lipid volume fraction, first the water volume fraction was calculated according to:

$$\varnothing_{aq} = \frac{c_{aq}}{c_{aq} + (1 - c_{aq})\left(\frac{\rho_{aq}}{\rho_{MAG}}\right)} \quad (1)$$

where $\varnothing_{aq}$ is the volume fraction of the aqueous portion (0.386 and 0.496 for fully hydrated $Q_{II}^{D}$phaseofMO and MPL respectively. and 0.416 and 0.584 when the dehydrated $Q_{II}^{G}$ phase is seen for MO and MPL respectively [64,67]), $c_{aq}$ is the water weight fraction, $\rho_{aq}$ denotes the density of water (0.997 g $cm^{-3}$), and $\rho_{MAG}$ represents the density of the MAG host lipid (0.942 g $cm^{-3}$ [68,69] for monoolein and 0.982 g $cm^{-3}$ for monopalmitolein) [70].

By subtracting the water volume fraction from 1, the lipid volume fraction $\varnothing_{MAG}$ was determined [68]:

$$\varnothing_{MAG} = 1 - \varnothing_{aq} \quad (2)$$

From there the lipid monolayer thickness ($l$) could be extrapolated [70]:

$$\varnothing_{MAG} = 2A_o\left(\frac{l}{d}\right) + \frac{4}{3\pi\chi\left(\frac{l}{d}\right)^3} \quad (3)$$

where $A_o$ and the Euler characteristic χ are constants specific to the type of bicontinuous cubic phase related to the minimal surface area given in Table 1, d is the lattice parameter determined by SAXS for the phase in nm, and l is the lipid chain length or thickness of the assembled lipid monolayer.

Ultimately, the radius of the congruent aqueous channels ($r_{aq}$) within the network was estimated utilizing the calculated lipid

**Table 1**
Surface area constants [70,71].

| | $A_o$ | $\chi$ |
|---|---|---|
| $Q_{II}^{D}$ | 1.919 | −2 |
| $Q_{II}^{P}$ | 2.345 | −4 |
| $Q_{II}^{G}$ | 3.091 | −8 |

chain length according to the following equation based on minimal surfaces [66,71]:

$$r_{aq} = \left(\sqrt{\frac{-A_o}{2\pi\chi}}\right)d - l \tag{4}$$

The area at the interface per lipid molecule in the unit cell of the cubic phase ($a_i$) was calculated directly according the following [70]:

First, the lipid molecular volume ($v_{MAG}$) was determined according to [68]:

$$v_{MAG} = \frac{\left(\frac{MW_{MAG}}{Avogadro's\ \ number}\right)}{\rho_{MAG}} \tag{5}$$

where $MW_{MAG}$ is the molecular weight ($g{\cdot}mol^{-1}$) for the host lipid, taken as 356.6 and 328.5 $g{\cdot}mol^{-1}$ for MO and MPL respectively.

From there, the area at the interface per lipid molecule was estimated according to the following equation:

$$a_i = 2v_{MAG}\frac{(A_o d^2 + 2\pi\chi l^2)}{\varnothing_{MAG} d^3} \tag{6}$$

where $A_o d^2 + 2\pi\chi l^2$is equal to the area at the head group at the interface integrated over a single monolayer

### 2.6. Enzyme stock preparation

A 5 mg/mL solution was prepared by dissolving the lipase in 0.1 M phosphate buffered saline (PBS), pH 7.4 ± 0.2. The preparation was carried out on ice to avoid denaturation or premature activation of the enzyme. Enzyme solutions were stored on ice or in the fridge and only used for up to one hour after preparation. New solutions were prepared for experiments thereafter. It is acknowledged that at this concentration, proteins displaying interfacial activity are prone to aggregation, however all samples were treated identically in this investigation under the same experimental conditions of enzyme exposure.

For the clofazimine salt, ultrapure water was substituted for the PBS in the preparation of the enzyme solution to prevent ion displacement from the citrate salt form of the API leading to reduced aqueous solubility [62].

### 2.7. Swelling and degradation behavior

To investigate the time-dependent swelling and degradation behavior of the lipid cubic phase gels prepared with different commercial lipids, pharmaceuticals and THL, dynamic swelling studies were performed. After sufficient equilibration the gels were weighed before submersion in 1 ml of phosphate buffered saline solution (pH 7.4 ± 0.2), both in the presence and absence of enzyme. The sample vials were tightly capped and maintained at 37 °C. The samples were shaken at 200 rpm throughout the investigation to ensure homogenous exposure of the sample to the enzyme. Porcine pancreatic lipase was selected for the study. For the clofazimine salt, ultrapure water was again substituted for the PBS to prevent ion displacement from the citrate salt form of the API leading to reduced aqueous solubility [62].

The swelling and degradation ratios of the gels were studied by means of a standard gravimetric method. The gels were removed from the media at regular intervals and their liquid uptake and mass loss was characterized by measuring the change in their mass. The gels were rinsed with purified MilliQ water to remove any residual salts potentially deposited on the surface of the gel from the swelling media and lipase solution debris. The excess surface water was then removed from samples by gentle blotting with lint-free Kimwipes™ before the samples were weighed on an analytical balance.

The swelling ratio and rate of degradation in terms of relative weight % were calculated against the initial sample mass as per the following equation:

$$Swelling\ Ratio\ or\ Residual\ Weight\ \% = \frac{W_1 - W_0}{W_0} \times 100\% \tag{7}$$

where $W_0$ is the initial gel weight before submersion in the media and $W_1$ is the weight of the gel at a measured time point after immersion in the media.

### 2.8. Drug release studies

The release of the model pharmaceuticals CFZ-citrate and caffeine from the LCP was tracked at timed intervals for up to 31 days in PBS or water for caffeine and CFZ-citrate respectively. Drug release measurements consisted of removing the entire solution from the sink and immediately replenishing it with fresh release media. Throughout the measurement, the samples were shaken at 200 rpm in an incubator at 37 °C. The concentration of CFZ-citrate and caffeine in the sink were measured by UV–vis spectrometry for CFZ-citrate and high performance liquid chromatography (HPLC) for caffeine, due to interference from the lipids in solution.

### 2.9. High performance liquid chromatography

The HPLC system used in this investigation was an Agilent 1200 Infinity Series (Agilent Technologies, Palo Alto, USA) comprising: G1311B 1260 quaternary pump, G1329B 1260 ALS autosampler, G1316A 1260 TCC (thermostated column compartment) and a G1365D 1260 MWD VL diode-array detector. The acquired data was processed with the Agilent OpenLAB CDS software.

Chromatographic separations of caffeine-containing samples were achieved using an Agilent Poroshell 120 PFP (3 × 100 mm, 2.7 μm) column fitted with a UHPLC Poroshell 120 guard module (3 × 5 mm, 2.7 μm). The system was maintained at 20 °C with a run time of 10 min. The mobile phase which comprised A: HPLC Analytical grade Acetonitrile (Fisher Scientific) and B: deionized water (A:B 15:85, v/v) was delivered to the column at a flow rate of 0.64 ml/min which yielded a column back pressure of ~290 bar. Samples were filtered through a 0.2 μm nylon filter (Fisherbrand®) and 8 μl injections were made. UV detection was conducted at a wavelength of 274 nm.

### 2.10. UV–visible spectroscopy

The concentration of CFZ citrate was determined by means of UV–vis spectrophotometry. A full spectrum was obtained on a double beam UV-1800 Shimadzu UV–Visible spectrophotometer to ascertain $\lambda_{max}$ for the drug, which was determined as 488 nm. Absorbance values of release samples were then obtained with appropriate dilution at this wavelength and Beer-Lambert's Law was then utilized to calculate the concentration of the API in the sample.

### 2.11. Drug release kinetics

The release data obtained for the release of caffeine and clofazimine citrate in the presence or absence of the THL inhibitor from the two MAG LCP formulations were treated according to a number of release models: zero-order (cumulative % drug released v time (min)); first order (Log cumulative % drug released v time (min)); Higuchi (cumulative % drug released v square root of time); Hixson-Crowell (cube root % total drug - cube root of % unreleased drug v time (min)); and Korsmeyer-Peppas (log cumulative % drug released v log time) to obtain the correlation coefficient. The diffusion coefficient (n) was estimated from the linear regression line of the Korsmeyer-Peppas model for each sample.

## 3. Results & discussion

### 3.1. Structural characterization of the mesophases

In this study, lipid cubic phases were successfully formed using monoolein and monopalmitolein in the presence of hydrophobic and hydrophilic pharmaceutical compounds as well as a lipase inhibitor, the chemical structures of which are shown in Fig. 1. Cubic phases are distinguishable by their discrete crystallographic space groups. Three inverse bicontinuous cubic phases exist; primitive ($Q_{II}^{P}$), gyroid ($Q_{II}^{G}$), and double-diamond ($Q_{II}^{D}$) with symmetry values of 229, 230, and 224 respectively. A range of characterization techniques can be applied in the distinction of these phases. This investigation utilized simple polarizing light microscopy and more thorough small-angle X-ray scattering approaches to assign mesophase properties to the test formulations. One can determine whether a test material is anisotropic or isotropic in nature and measure its birefringence simply by using cross-polarized microscopy (CPLM) [72]. As the highly ordered cubic phase exhibits optical isotropy and its refraction is non-birefringent in nature, it gives rise to a dark background between crossed polars as the phase is essentially 'invisible' against the dark stage [73]. The lamellar and hexagonal liquid crystalline phases on the other hand, are anisotropic and optically birefringent thus split the plane of the incident light appearing as textured multi-coloured patterns. This distinction allowed for the identification of the phases of our formulations. Indeed, when the fresh formulations under investigation in this study were exposed to cross-polarized light, a dark image was observed with no obvious signs of birefringence suggesting a structure of cubic architecture.

While CPLM allows for differentiation between mesophases, its usefulness is limited by an inability to distinguish between the various types of discrete cubic phases and it provides no means for dimensional analysis. Small angle X-ray scattering investigations enabled the lattice dimensions and unambiguous space group symmetry to be assigned to each sample. They also allowed for the effect of THL and API loading on the phase properties, and its impact on the stability of the phase to be tracked. With a favorable effect in terms of stability against lipolytic enzymes anticipated, phase identification was required to confirm the loading capabilities of the MAG LCP systems. Lipid cubic phases typically give rise to diffraction patterns similar to those of powder X-ray diffraction; characterized by a series of sharp, clearly defined concentric rings owing to their randomly orientated domains of cubic symmetry [10]. Fig. 2 shows the 1D azimuthally integrated SAXS patterns of freshly made MAG LCP systems of MO and MPL. Bragg peaks have been indexed according to the Miller indices of the reflection plane to assign the mesophase. The relative positions of the reflection lines indicated the presence of highly ordered bicontinuous cubic phases in our samples. The MAG-water system typically accesses two types of cubic phase under equilibrium at room and body temperature depending on the level of hydration [18]. At lower water concentrations the gyroid or '$Q_{II}^{G}$ ' cubic phase is accessed and when hydration levels are increased the phase transitions to the more swelled and stable diamond cubic ($Q_{II}^{D}$) phase. The $Q_{II}^{D}$ phase is stable against dilution and maintains its architecture when the water content is increased further to excess levels. As expected, in all of the systems for both host lipids, the phase in equilibrium with excess water was of the cubic-$Q_{II}^{D}$ type with lattice parameters (Table 2) slightly higher than those referenced in the literature [74,75]. The estimated water channel diameter dimensions however (Table 2) were in agreement with published values [13,26] with larger values for channel diameter estimated for the MPL system as expected [67].

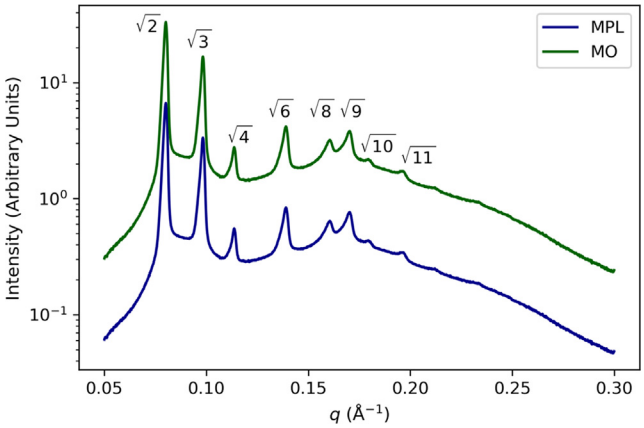


**Fig. 2.** 1D azimuthally integrated SAXS patterns of fresh monoolein (MO) and Monopalmitolein (MPL) of blank cubic mesophases. The peaks of both patterns have been indexed according to the $Q_{II}^{D}$ mesophase. Repetitions (see supplementary information) demonstrated no impact on the mesophase from radiation damage.

Samples prepared below excess hydration levels saw a transition from the $Q_{II}^{D}$ to $Q_{II}^{D}$ + $Q_{II}^{G}$ that occurred across all specimen, even in those prepared fresh on the day of testing (data not shown). In these dual-phase regions, the individual lattice parameter of the respective phases should remain constant with little influence from the sample make-up as a whole. In Table 2, the transition from a single phase to the co-existence of two bicontinuous cubic phases in the monoolein/water system is seen as dehydration of the sample occurs [18,64], likely occurring during transferal to the sample stage and also during storage [76]. It is also possible that the fresh formulations had not yet fully equilibrated to a homogeneous hydration state at the time of testing, which could explain the coexistence of two cubic phases. The coexistence between the $Q_{II}^{D}$ and $Q_{II}^{G}$ is supported by the Bonnet ratio between the lattice parameters: the ratio of unit cell dimensions of coexisting cubic phases related through Bonnet transformations [77]. In the case of coexistence between $Q_{II}^{D}$ and $Q_{II}^{G}$ mesophases, the Bonnet ratio should be 1.57. It should also be noted at this point, that in utilizing X-rays for sample research, the impact of radiation damage on any given specimen, especially those soft biomaterials such as lipid mesophases, is a justified concern. However, the work of Cherezov and colleagues attests that the radiation dosage and exposure time used in this investigation is not likely to have a significant impact on the MAG mesophases under examination [78]. Here, 15 frames per sample recorded sequentially in one single location were analyzed and no significant difference was observed in the series plots (supplementary information).

Table 2 reports the mesophases assigned for samples doped with varying concentrations of THL, the lipase inhibitor, up to 2.5 wt% obtained from SAXS experiments using Eqs. (1) through

**Table 2**
Phase identification and lattice parameters of assigned mesophases at varied THL loadings from SAXS experiments with estimated dimensional values for lipid chain length (L) and water channel diameter ($D_{H2O}$). Samples assigned F were made fresh on the day of SAXS experiments.

| Host Lipid | THL (wt. %) | Storage (days) | mesophase | Lattice Parameter (nm) | L (nm) | $D_{H2O}$ (nm) | Bonnet ratio (where applicable) |
|---|---|---|---|---|---|---|---|
| MO | 0 | F | $Q_{II}^{D}$ | 10.17 | 1.74 | 4.48 | – |
| MO | 0 | 21 | n/a* | – | – | – | – |
| MO | 0.7 | F | $Q_{II}^{D}$ | 9.92 | 1.69 | 4.37 | – |
| MO | 1.5 | F | $Q_{II}^{D}$ | 9.6 | 1.64 | 4.23 | – |
| MO[CE] | 1.5 | 21 | $Q_{II}^{D}$ | 9.63 | 1.65 | 4.23 | 1.49 |
| | | 21 | $Q_{II}^{G}$ | 14.34 | 1.43 | 4.25 | |
| MO | 2.5 | F | $Q_{II}^{D}$ | 9.24 | 1.58 | 4.06 | – |
| MPL | 0 | F | $Q_{II}^{D}$ | 10.8 | 1.48 | 5.48 | – |
| MPL | 0 | 21 | n/a* | – | – | – | – |
| MPL | 0.7 | F | $Q_{II}^{D}$ | 10.47 | 1.43 | 5.32 | – |
| MPL | 1.5 | F | $Q_{II}^{D}$ | 9.96 | 1.36 | 5.06 | – |
| MPL[CE] | 1.5 | 21 | $Q_{II}^{D}$ | 10.38 | 1.42 | 5.28 | 1.56 |
| | | 21 | $Q_{II}^{G}$ | 16.20 | 1.62 | 4.79 | |
| MPL | 2.5 | F | $Q_{II}^{D}$ | 9.88 | 1.35 | 5.03 | – |

[CE] Samples that presented the coexistence of two mesophases.
* One single peak detected i.e. no mesophase; storage time of sample in sealed vial prior to SAXS.

(4). The formulations of both MO and MPL at increasing concentrations of THL present cubic structures almost identical to those of the blank matrices. Fig. 3 shows the effect of incorporating increasing concentrations of the hydrophobic THL in MAG LCP systems of MO and MPL on the SAXS patterns. The addition of the lipase inhibitor appeared to bear no major effect on the peak positioning with only minor shifts in scattering vector q observed. The integrated SAXS patterns demonstrated how increasing the concentration of the THL lipstatin saw a shift towards higher q for the LCP systems. This is directly related to the swelling of the phase; with higher q indicating a smaller lattice parameter of the mesophase. The lattice spacing and space group assignment provide a metric for the estimation of cubic phase structural dimensions, which can aid in host lipid selection and loading capacity determination. The volume fraction of the lipid component along with d-spacing values were essential parameters in estimating the internal dimensions of the mesophases [70]. Values pertaining to the structural dimensions of the cubic formulations were estimated utilizing these parameters as well as the phase identity obtained from the SAXS experiments according to Eqs. (1) through (4). In bicontinuous cubic phases, under conditions of equilibrium, the characteristic lattice spacing is directly related to the diameter of its penetrating water channels; and an increase in parameters is observed with increasing hydration. This increase is seen only within certain limits [64].

In the case of the monoolein LCP system, the amount of the hydrophobic THL added appeared to be inversely related to the aqueous channel diameter; reducing by a little over 0.4 nm as the weight percent of THL increased from 0 to 2.5% w/w, Table 2. A decrease in water channel diameter is also evidenced by higher q values as shown in Fig. 3. This coincided with a slight reduction in lattice parameter for these samples. A similar relationship was seen in the LCP systems prepared with the shorter chain monopalmitolein host lipid whereby an increase in THL loading saw a reduction in both the water channel diameter and lipid layer depth. Indeed, the reduction in this case was slightly higher than that in the MO 9.9 MAG monoolein system, with a reduction of almost 0.5 nm observed.

The impact of THL on the stability of the LCP systems over time was also investigated where the metastability of the phase structure over 3 weeks was studied. Diffraction patterns were examined in relation to those samples freshly prepared on the day of testing. A phase transition, similar to that observed in the samples prepared below excess hydration, was seen in those samples stored over a 3 week period when prepared with the inhibitor; where

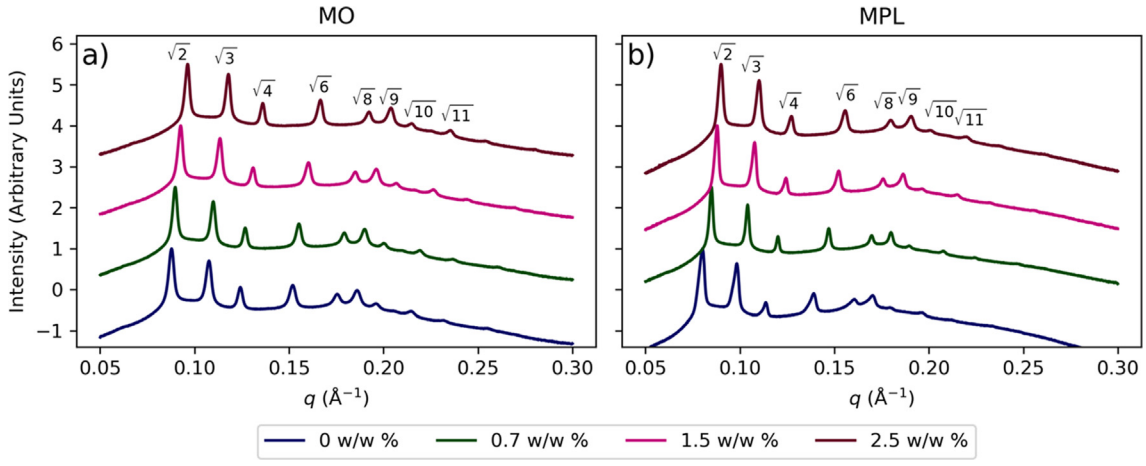


**Fig. 3.** Azimuthally integrated SAXS patterns of monoolein (MO, a) and monopalmitolein (MPL, b) mesophases doped with increasing concentrations of THL from 0 (fresh) – 2.5 w/w %. The patterns have been indexed according to the $Q_{II}^{D}$ mesophase.

peak broadening and the co-existence of two cubic systems ($Q_{II}^{D}$ + $Q_{II}^{G}$) was presented (Fig. 4(a) and (b)). However, in samples prepared without the THL, the initial phase transitioned even further beyond the liquid crystalline region entirely, highlighting the stabilizing effect of the THL inhibitor on the LCP mesophase. Smooth, sharp diffraction rings corresponding to discrete cubic phase symmetry are highlighted in the 1D azimuthally integrated SAXS patterns for the fresh samples in Fig. 4(a) and (b).

The observed increase in stability of the MAG LCP systems over time owed to the presence of the inhibitor may be related to changes in the packing frustration of the phases. When considering the phase behavior of pure monoacylglycerols such as MO and MPL, there are really only two major influential parameters at play – temperature and water content. However, when you venture outside of pure lipid systems and begin to consider how their behavior is affected or driven by other compositional factors such as the inclusion of additive molecules, one might find that the phase behavior changes, potentially deviating from their classical binary behavior. The impact of introducing a third contributing factor stretches the system beyond this simplistic model to a much more complex ternary system [79]. The introduction of hydrophobic molecules in particular has been shown to induce changes on the molecular level, subsequently altering the morphology of the phase. These studies described the effect on packing frustration (the energy cost associated with deviation from the favored shape in a particular phase) of MO cubic phases induced by the addition of a hydrophobic long chain alkane tricosane [80]. They have demonstrated the relationship between the packing frustration and cubic phase stability, whereby the introduction of the hydrophobic molecules reduced the frustration by partitioning into the hydrocarbon chain domains [81,82], subsequently stabilizing the mesophase [83]. The stabilizing effect may also be explained by an interaction between the hydrophilic moieties of the tetrahydrolipstatin molecule and the water present in the penetrating channels. It is possible that hydrogen bonding between water and the carbonyl or amide groups of THL, Fig. 1, could retain water molecules in the matrix, thus maintaining the cubic phase over the three week storage period investigated, where dehydration of the blank systems resulted in the disassembly of the mesophase. More thorough SAXS investigations into the exact location of the inhibitor in the phase would be required to corroborate this theory.

Ultimately, the objective of this study was to control the rate of release of hydrophobic drugs from LCP systems. To assess the suitability of the THL-containing LCP systems as controlled drug delivery matrices, two model pharmaceutical agents (caffeine and CFZ-citrate salt) were selected based on their propensity to dissolve in water. Samples were prepared with increasing amounts of both APIs (1 and 3 wt%) in a bid to establish the carrying capacity of the cubic phase for APIs located in different regions of its network. The resulting mesophases and their corresponding dimensional estimations are shown in Table 3. As with samples without added API, coexistence between $Q_{II}^{D}$ and $Q_{II}^{G}$ mesophases is supported by the Bonnet ratio.

The incorporation of the hydrophobic CFZ citrate salt into the lipid matrices lead to an increase in the lattice parameter, and the width of the water channels. This effect was more pronounced in the case of the upper loading of 3 wt% API. In the MPL system, the coexistence of a second double diamond cubic phase structure is observed with larger structure parameter values at both API loadings (+0.91 to 1.32 Å). In the MO LCP-THL system, a phase coexistence was observed, with reduced water channel diameter and shift to higher q (Å) noted. The incorporation of hydrophilic caffeine at 1 wt% loading into the MO LCP formulations did not significantly affect the lattice parameter and size of water channels. The relatively small size of the molecule (0.243 $nm^3$) [84] meant that it could be easily accommodated in the aqueous channels (4.48 ± 0.03 and 5.48 ± 0.13 nm in MO and MPL LCP respectively, shown as the mean value of 3 samples ± standard deviation) of the matrix and therefore the $Q_{II}^{D}$ structure was preserved. The presence of the caffeine (1 wt%) in the 1.5 wt% THL LCP system left the phase seemingly unaffected, with a single $Q_{II}^{D}$ space group maintained for both MO and MPL host lipid LCPs that were comparable to the blank systems. It is clear that the structural parameters of the $Q_{II}^{D}$ regions are greater than those of the $Q_{II}^{G}$. This is expected as the $Q_{II}^{D}$ phase is accessed at a higher hydration point than the $Q_{II}^{G}$ region, which in turn influences the physical dimension of the unit cell [18,64]. The presence of an unassignable peak between 0.134 and 0.136 $Å^{-1}$ in the MO samples containing the caffeine API may be owed to API precipitation or formation of a caffeine hydrate in the system as the sharp Bragg peak was not observed in the blank system and could not be assigned to any mesophase. Its presence does however elude to the existence of a crystal of some sort.

The release kinetics of the cubic phase are governed by the phase identity and the capacity of its aqueous channels. In addition

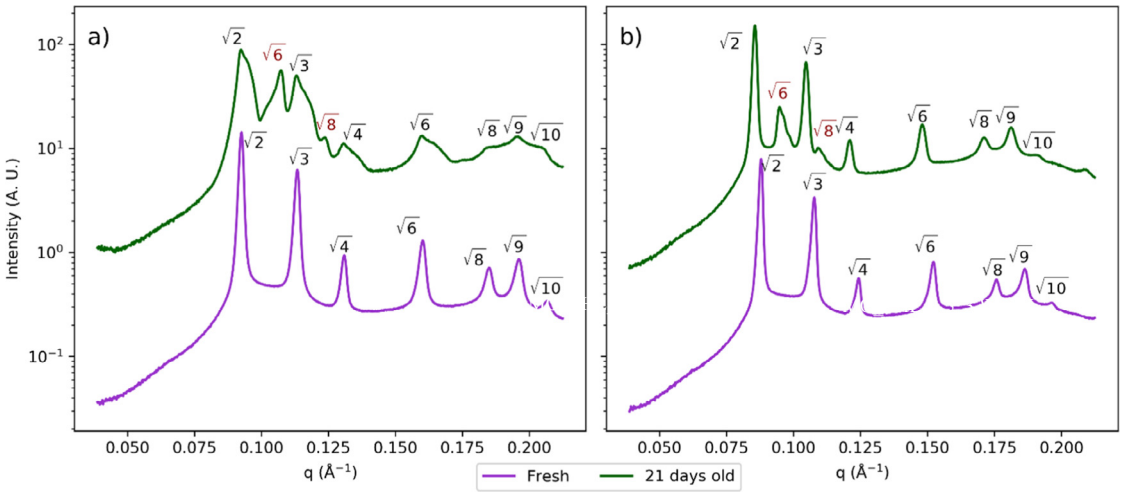


**Fig. 4.** The effect of incorporating the hydrophobic THL lipstatin on the stability of monoolein (a) and monopalmitolein (b) lipid systems over 3 weeks at 37 °C. Bragg peaks have been indexed according to the Miller indices of the reflection plane to assign mesophase. 1D azimuthally integrated SAXS patterns of blank mesophases and those doped with 1.5 w/w % THL in order of decreasing storage time prior to analysis. The patterns have been indexed to either the $Q_{II}^{D}$ (black text) or $Q_{II}^{G}$ (red text) mesophase.

**Table 3**
Phase identification and lattice parameters of assigned mesophases for varied THL and model API loading from SAXS experiments with estimated dimensional values for lipid chain length (L) and water channel diameter ($D_{H2O}$).

| Host Lipid | THL (wt. %) | API | Storage (days) | mesophase | Lattice Parameter (nm) | L (nm) | $D_{H2O}$ (nm) | Bonnet ratio (where applicable) |
|---|---|---|---|---|---|---|---|---|
| MO[CE] | 0 | CFZ 3% | 2 | $Q_{II}^{D}$ | 10.74 | 1.83 | 4.73 | – |
| | | | 2 | $Q_{II}^{D}$ | 9.55 | 1.63 | 4.21 | |
| MO[CE] | 1.5 | CFZ 1% | 2 | $Q_{II}^{D}$ | 8.89 | 1.52 | 3.90 | 1.58 |
| | | | 2 | $Q_{II}^{G}$ | 14.01 | 1.85 | 3.25 | |
| MPL[CE] | 0 | CFZ 1% | 2 | $Q_{II}^{D}$ | 11.12 | 1.52 | 5.65 | – |
| | | | 2 | $Q_{II}^{D}$ | 12.44 | 1.71 | 6.31 | |
| MPL[CE] | 0 | CFZ 3% | 2 | $Q_{II}^{D}$ | 9.65 | 1.32 | 4.90 | – |
| | | | 2 | $Q_{II}^{D}$ | 10.56 | 1.44 | 5.37 | |
| MPL[CE] | 1.5 | CFZ 1% | 2 | $Q_{II}^{D}$ | 10.62 | 1.46 | 5.38 | – |
| | | | 2 | $Q_{II}^{D}$ | 11.84 | 1.62 | 6.01 | |
| MO | 0 | Caff 1% | 2 | $Q_{II}^{D}$ | 10.07 | 1.72 | 4.43 | – |
| MO | 0 | Caff 3% | 2 | $Q_{II}^{G}$ | 15.09 | 1.99 | 3.50 | – |
| MO | 1.5 | Caff 1% | 2 | $Q_{II}^{D}$ | 9.71 | 1.66 | 4.27 | – |
| MPL[CE] | 0 | Caff 1% | 2 | $Q_{II}^{D}$ | 11.75 | 1.61 | 5.96 | 1.54 |
| | | | 2 | $Q_{II}^{G}$ | 18.11 | 1.81 | 5.36 | |
| MPL[CE] | 0 | Caff 3% | 2 | $Q_{II}^{D}$ | 11.82 | 1.62 | 5.99 | 1.53 |
| | | | 2 | $Q_{II}^{G}$ | 18.11 | 1.81 | 5.36 | |
| MPL | 1.5 | Caff 1% | 2 | $Q_{II}^{D}$ | 10.46 | 1.43 | 5.32 | – |

*One single peak detected i.e. no mesophase; storage time of sample in sealed vial prior to SAXS.
[CE] Samples that presented the coexistence of two mesophases.

to the effect the physio-chemical properties of the matrix itself have on the diffusion of the API, the properties of the API being incorporated also influence the transport properties of the matrix and have been reported to induce phase transformations upon formulation [4,13,66]. It is therefore imperative to ensure that the incorporated API does not disrupt the assembly of the cubic phase lattice structure which may in turn affect its function. In some cases, this may limit the use of the cubic phase as a drug delivery matrix. While some dimensional changes in the crystallographic unit cell were observed upon the incorporation of both model drugs, the conclusion was drawn that the molecular distribution of the lipid cubic phases was not significantly altered by their presence at concentrations below 3 wt%. Additionally, the incorporation of the lipase inhibitor THL did not induce a phase transition and both systems have shown the ability to preserve the cubic structures at room temperature; showing only a small increase of the crystallographic unit cell parameter. This is important as major changes in the phase properties, or transitions out of the cubic region caused by the incorporation of an API, may render the system unsuitable for certain applications as their release kinetics are governed by the mesophase of the lipid delivery system.

### 3.2. Swelling and degradation

As previously discussed, the integrity of lipid cubic systems, especially those generated from MAG host lipids, is vulnerable in the presence of a family of enzymes referred to as lipases [85]. This in turn may directly impact the release of the APIs that it encapsulates. In humans three major lipases exist, where their role is in the digestion and catabolism of dietary fatty intake [54,86,87]. The lipase family of enzymes display significant sequence homology between species and this investigation utilized a model lipase from porcine pancreas to which tetrahydrolipstatin has the ability to bind and inhibit through irreversible interactions [88]. The lipolysis of the cubic phase in solution was followed both visually and gravimetrically. At predetermined time points, the mass of the gel was measured and the residual weight % was calculated (Eq. (7)). The degradation could also be tracked visually, and its initiation was indicated by the formation of an off-yellow oil layer on the outer surface of the gel. The digestion eventually resulted in an entirely cloudy solution with the oily layer sitting on top.

For both MAG LCP systems, those exposed to lipolytic enzyme in the incubation medium saw a rapid decline in original mass for the blank MAG lipid cubic systems compared to those incubated in enzyme-free PBS buffer. The integrity of the MO LCP was compromised, and the enzyme action broke down the entire gel after a 7 day exposure. The gel that was spared lipase exposure maintained almost half of its original mass over a testing period of 12 days. Similarly, in the MPL LCP system, the gel maintained 94 ± 0.53% of its original mass after 17 days in the enzyme free buffer, while the cubic gel exposed to lipase was digested to its oleic acid and glycerol components over the course of 10 days. In fact, the gel incubated in lipase-free buffer was subject to a loss of only 13 ± 2.5% over a testing period of 36 days.

Tetrahydrolipstatin is a potent lipase inhibitor and the lipophilic molecule exerts its inhibitory effect upon binding the pancreatic lipase at its serine active site as previously mentioned in the introduction to this study. THL was incorporated into cubic formulations generated from both host lipids at increasing concentrations to study its effectiveness in impeding their lipolysis. Concentrations of 0.35, 0.7, 1.5 and 2.5 wt% were chosen to study the potential tunability of the systems in terms of the LCP lifespan compared to the blank systems as a means of further controlling the rate of release of hydrophobic APIs in particular, which is concomitant with hydrolytic digestion.

Fig. 5 (a) shows the enzyme-driven hydrolysis of the monoolein LCP gels, both with and without THL up to 2.5 wt% embedded in its network. Increasing the concentration of the THL in the lipid network incrementally decreased the degradation rate of the gels by almost 6 fold at the highest loading compared to the LCP without inhibitor. Even at the lowest inhibitor concentration (0.35 wt%), the loss in original mass was slowed down and the systems maintained 49.7 ± 9.5% of their original mass after 7 days when the blank LCP had been fully digested into their soluble oleic acid and glycerol components.

A control group was also studied, where MO LCP was incubated with lipase and free THL in solution at a concentration of 1.5 mg/mL. Here, an increase in stability was observed as the samples were fully degraded after 15 days compared to the degradation rate of

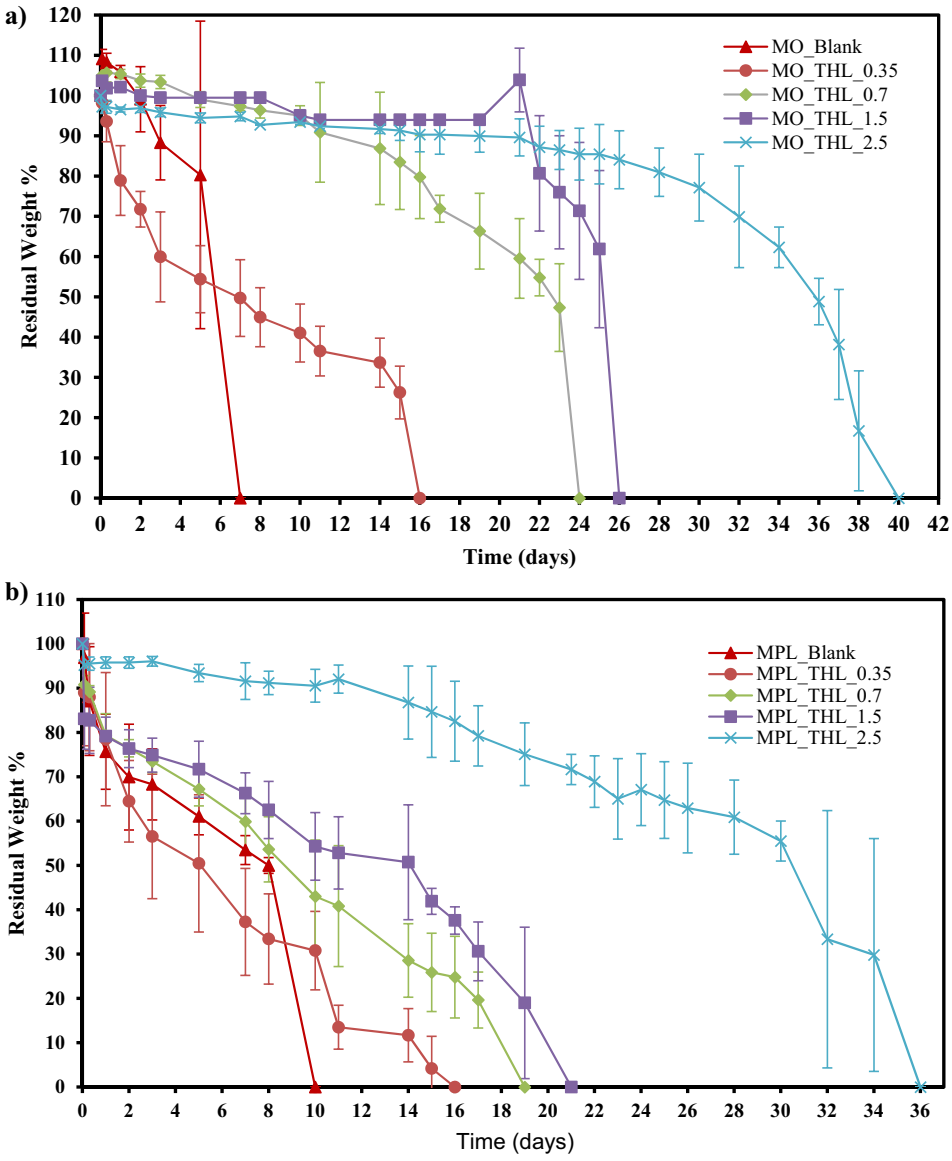


**Fig. 5.** Swelling and degradation profile of: a) Monoolein and b) Monopalmitolein LCP formulations (Blank or formulated with THL) in Physiological Buffer (1X PBS) incubated at 37 °C in the presence of lipase enzyme. Each point represents a mean value ± standard deviation of three determinations.

the MO LCP with lipase, where they had fully degraded by day 7. The rapid loss in mass may have occurred as a result of a combination of phase change and mass depletion rather than solely the lipolysis of the lipid component itself. In this control group, the THL in solution was replenished with each change of media at least every 24 h, and yet the MO LCP with the THL incorporated into its network displayed greater stability and did not fully degrade until day 24. These latter samples only had the initial 1.5 mg/ml of THL added for the duration the experiment and the depletion in mass occurred with little initial swelling observed, possibly on account of the hydrophobic effect of the membrane bound inhibitor pointing towards a predominantly surface-driven digestion pattern.

The same experimental conditions were tested on the MAG LCP of slightly shorter chain length (just 2C shorter), monopalmitolein, Fig. 5 (b). Once again, an increase in stability was noted in the presence of the THL, even at the lowest loading of 0.35 wt% where the LCP samples maintained between ~31 and 33% of their original mass at 10 days by when the blank gels were completely broken down. There was no observed swelling between tested timepoints indicating that the diffusion of enzyme solution into the phase did not outpace the degradation. The 0.35 wt% samples were not fully digested until after 15 days in incubation.

Both systems were considered to be comparable in terms of tunable stability, and for the majority the error, while still relatively small, between samples may be generally explained by the variation in distribution of the lipstatin between gel formulations. Although all samples were prepared following identical protocols of manual and vortex mixing, the hydrophobic inhibitor is suspended rather than dissolved within the formulation and is likely not completely homogeneous. While the two LCP systems appear to follow similar digestive trends, the incorporation of the THL showed a more prolonged stability period in the MO LCP versus the MPL system compared to the samples prepared without the inhibitor in their respective profiles. This difference may be attributed to the difference in water channel diameters and lipid packing described already in the SAXS section of this investigation, where the wider diameter of aqueous channels in the MPL system allowed for a higher penetration of the external lipase solution into the phase's aqueous network, in turn speeding up the degradation process. The SAXS data clearly showed a lower degree of swelling

of MO LCP in the presence of THL under conditions of excess water (shown by higher q values) suggesting that lower volumes of lipase solution could penetrate and diffuse into the phase.

The faster degradation of the MPL LCP system may therefore be attributed to the higher surface area associated with the lipid portion of the phase. The interfacial area per lipid molecule of both MAG LCP systems was estimated using Eqs. (5,6) which utilized the lattice parameter and calculated lipid chain length obtained from the SAXS data. The calculated surface area was shown to be larger in the shorter chain MPL system (Table 4). This provides the lipase with a larger access area at the interface required for it to carry out its lipolysis. On the contrary, the surface area is seen to increase as the water channel diameter decreases with higher THL loadings. Despite this, the degradation is clearly slowed down by the THL's presence which may seem counter-intuitive. It is however hypothesized that with the larger associated surface area of the lipid portion, comes greater inhibitor exposure at the interface where lipase acts.

Once again, the digestion of the LCP samples was easily trackable upon visual inspection. After prolonged lipase exposure, the sample appearances became cloudier in colour, with a brittle core covered in a more viscous outer layer. The samples prepared with the inhibitor maintained the characteristically clear colour of the lipid cubic phase for longer than those blank samples; with the change in appearance noted after only 3 days in incubation for the blank gels compared to 7 days in the doped gels.

To confirm that the THL-containing samples maintained the cubic phase as well as the system mass in the presence of the lipase solution, LCP samples were prepared for both host lipid systems with and without THL at 1.5 wt% incorporated into the membrane and were exposed to lipase solution for 3 days before SAXS analysis was conducted. In both cases, the $Q_{II}^{D}$ structure was preserved despite a reduction in mass noted for the samples prepared in the absence of THL (Table 5).

In the more readily digested MPL system in the absence of THL, the SAXS data demonstrated a transition of the LCP to what appears to be a hexagonal phase ($H_{II}$) within the network after exposure to the lipase. It is described in the literature that both the instinctive formation of the phase and the thermodynamic stability of the LCP are driven by an opposition between a pair of free energy terms. When this competition between the curvature energy of the individual monolayers and stretching energy of the lipid chains exists in its least frustrated state, it is suggested to be responsible for the nature of the solid state phase and its position on the phase diagram [71]. The hexagonal phase comprises an arrangement of limitless water rods divided by lipid bilayers in a two dimensional lattice and the transition to the phase upon lipase interaction has previously been reported where the presence of the lipase in solution served to increase the curvature of the system, subsequently altering the molecular structure inducing a phase transition [35,89]. This was not seen in the MO system although the presence of a second $Q_{II}^{D}$ lattice was noted where only one existed in the sample containing the inhibitor. The same phenomenon was seen in the MPL system even in the sample formulated with the inhibitor.

From the stability tests conducted in the presence of lipase, it may be possible to control the duration of the prolonged release of hydrophobic molecules from LCP matrix networks using lipase inhibitors, allowing for the selection of the most suitable system for a given clinical drug delivery application. Fig. 6 shows stability plots for both of the LCP-inhibitor formulations; where increasing THL concentration was plotted against the stability of the phase in lipase solution. These models may provide researchers with a mode of predicting the phase stability against lipase digestion up to 40 or 36 days for the MO- and the MPL- THL LCP systems respectively across a range of inhibitor concentrations from 0 to 2.5 wt%.

### 3.3. Drug release studies

Numerous approaches have been described to modulate the kinetics of drug release to systematically control or prolong the drug delivery period of hydrophilic agents [4,10,90–92]. In this study, we sought to investigate the impact of addressing the rate of degradation of the phase as a means to control the release of

**Table 4**
Calculated interfacial area per lipid molecule ($a_i$) of MAG LCP generated at different THL loadings.

| Host Lipid | THL % | Storage (days) | mesophase | $a_i$ ($nm^2$) |
|---|---|---|---|---|
| MO | 0 | F | $Q_{II}^{D}$ | $3.13 \times 10^{-22}$ |
| MO | 0.7 | F | $Q_{II}^{D}$ | $3.22 \times 10^{-22}$ |
| MO | 1.5 | F | $Q_{II}^{D}$ | $3.32 \times 10^{-22}$ |
| MO | 2.5 | F | $Q_{II}^{D}$ | $3.45 \times 10^{-22}$ |
| MPL | 0 | F | $Q_{II}^{D}$ | $3.43 \times 10^{-22}$ |
| MPL | 0.7 | F | $Q_{II}^{D}$ | $3.54 \times 10^{-22}$ |
| MPL | 1.5 | F | $Q_{II}^{D}$ | $3.73 \times 10^{-22}$ |
| MPL | 2.5 | F | $Q_{II}^{D}$ | $3.75 \times 10^{-22}$ |

**Table 5**
Phase identification and lattice parameters of assigned mesophases for varied THL loading exposed to lipase from SAXS experiments.

| Host Lipid | THL (wt. %) | Storage (days) | Mesophase | Lattice Parameter | L (nm) | $D_{H2O}$ (nm) |
|---|---|---|---|---|---|---|
| MO[CE] | 0 | 3 | $Q_{II}^{D}$ | 10.64 | 1.81 | 4.69 |
| | | | $Q_{II}^{D}$ | 9.66 | 1.65 | 4.25 |
| MO | 1.5 | 3 | $Q_{II}^{D}$ | 9.68 | 1.65 | 4.27 |
| MPL[CE] | 0 | 3 | $Q_{II}^{D}$ | 10.56 | 1.45 | 5.36 |
| | | | $H_{II}$ | 9.35 | – | – |
| MPL[CE] | 1.5 | 3 | $Q_{II}^{D}$ | 10.31 | 1.41 | 5.24 |
| | | | $Q_{II}^{D}$ | 9.35 | 1.28 | 4.75 |

L is the lipid chain length/monolayer thickness (nm); $D_{H20}$ is the diameter of the water channels (nm).
[CE] Samples that presented the coexistence of two mesophases; storage time of sample in sealed vial prior to SAXS.

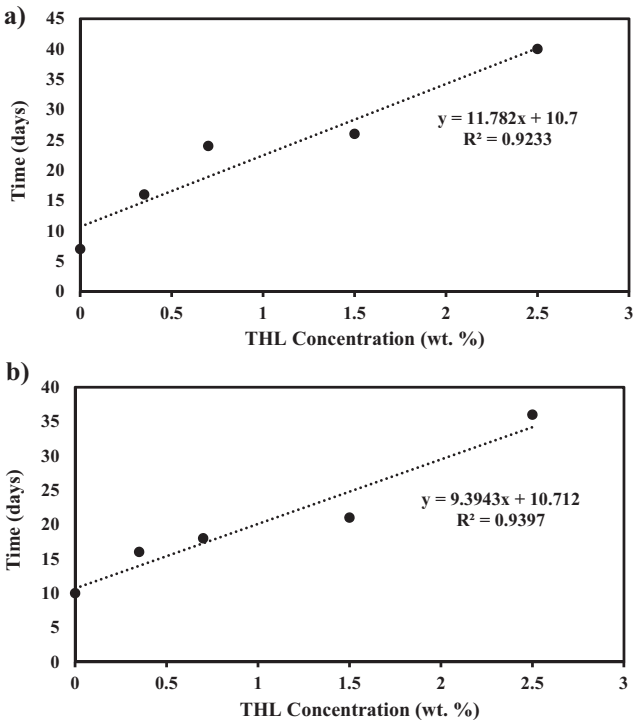


**Fig. 6.** Stability plots for a) MO-THL and b) MPL-THL LCP-inhibitor systems showing increasing THL concentration plotted against the stability (days) of the cubic phase in lipase solution.

model APIs. We were particularly interested in its impact on hydrophobic pharmaceuticals. It was hypothesized that the incorporation of the inhibitor would have greater influence on the predicted degradation-driven release of hydrophobic agents and little to no effect on more water-soluble molecules.

Clofazimine (CFZ), an antimycobacterial agent indicated for the treatment of leprosy, was selected as a model drug on account of its Biopharmaceuticals Classification System (BCS) class II properties of low aqueous solubility. Our group has previously developed a number of novel salt forms of clofazimine in a bid to improve the uptake of the drug *in vivo* [62]. One of these salts, co-formed with a citrate ion, was selected for this study on account of its enhanced aqueous solubility (~40 mg/L) which made studying its release possible. Not only that, but the API itself has shown high uptake in micelles and liposomes [93] and so its highly lipophilic nature [94] render CFZ a perfect subject to profile the release of membrane anchored molecules from our LCP-inhibitor systems.

The release of CFZ-citrate from the MAG systems, with and without THL and in the presence of lipase at 37 °C, is displayed in Fig. 7. Upon initiation of significant digestion of the LCP matrices after approximately 24 h in both systems in the absence of the inhibitor, CFZ-citrate release appears to be inversely proportional to the residual mass of the matrix. In the case of lipophilic APIs such as CFZ citrate which are thought to be predominantly located in the lipid bilayer, the rate of their diffusion is believed to be limited by their partitioning into the bilayers and is controlled by the erosion and breakdown of the carrier [28]. The release of the CFZ salt was found to be slower in the MO-based LCP compared to the MPL system under identical conditions. This result was expected from the faster degradation observed for MPL (Fig. 5) in the absence of THL and presence of lipase, where the gel was entirely digested into its core constituents. The oil layer maintained the characteristic red colour of the CFZ indicating that some of the API remained bound to the lipid digestion products at the end of the LCP gel degradation.

The influence of THL on the dissolution profiles is also clearly represented in Fig. 7 compared to the samples without the inhibitor; showing the prolonged release of the hydrophobic model drug upon its addition to the mesophases. The release rates were significantly slower in the systems that had the THL in their network with less than 20% cumulative release in both host lipid formulations after the testing period, indicating that its incorporation can control the rate at which the drug is eliminated from the gels. As discussed, this control is believed to be owed to the interaction of the THL with the lipase, thus inhibiting the degradation of the cubic mesophase. In the absence of the inhibitor, the lipase acts at the lipid/water interface to breakdown the matrix into an oily emulsion enabling the CFZ-citrate to partition into the media while this effect is delayed by the presence of the THL.

In the MO system formulated with 1.5 wt% THL, the CFZ salt continued to be released into solution at a steady rate over a 3 week testing period. After a 21 day incubation at 37 °C and 200 rpm approximately 25% of the drug was released. 40% of the original CFZ salt loading in the MPL-THL system was released from the bulk phase after this period. The MO-based gel mass had not reduced beyond 20% of its original weight and the MPL system maintained almost 60% of its original mass after this time. These results highlight the influence of tunable degradation of the cubic phase on controlled release of hydrophobic agents.

The release data for these hydrophobic API systems was fitted to a number of theoretical and empirical drug release models to study the effect the incorporation of the inhibitor had on controlling the release of CFZ-citrate (supplementary information). The literature indicates the Korsmeyers-Peppas, first-order kinetics and Higuchi models as the most representative of release from cubic phases [74]. These mathematical models, among others, were applied. However, in this case, the release data did not appear to fit well with these fundamental models described, although the best fit was indeed seen with zero-order and Korsemeyer-Peppas release kinetics indicating an anomalous non-Fickian diffusion transport that is both diffusion and swelling/erosion controlled. In examining the coefficient values (n) obtained for the CFZ salt from the Korsemeyer-Peppas model, we saw values pointing towards non-Fickian case 2 relaxation or super-case transport-2 mechanism ($n > 0.45$) on account of the hydrophobic salt's location in the lipid membrane. This supported the theory that erosion was a driving force in its release [74]. In both cases, higher coefficient values were observed in the gels without the inhibitor, where significant degradation was observed over the testing period directly related to the release of the drug into solution. These values elude to deviation from straight-forward diffusive transport and the results reiterate the influence the swelling and erosion of the matrix has on release of CFZ and serves to further affirm the concept of targeting degradation as a reasonable approach to extend the control inherently offered by the cubic phase itself without altering its phase structure.

While it is generally accepted that release of APIs from bioerodible polymers, such as lipid-based systems, is biphasic, driven by both diffusion and matrix effect [37], it is clear from the model plots and the respective $r^2$ values obtained (supplementary information) that the release from these LCP-inhibitor formulations is not simplistic, nor two-dimensional. While these mathematical models provided us with an indication of the release kinetics at play, there are several influential factors in this ternary system that drive the liberation of the hydrophobic API from its network. This makes it difficult to apply the existing simplistic mathematical models to its release, most of which assume a spherical-shaped system, which of course is not this case here. The release profile is, without dispute, complex with a combination/opposing effect of the variables on water uptake and digestion responsible.

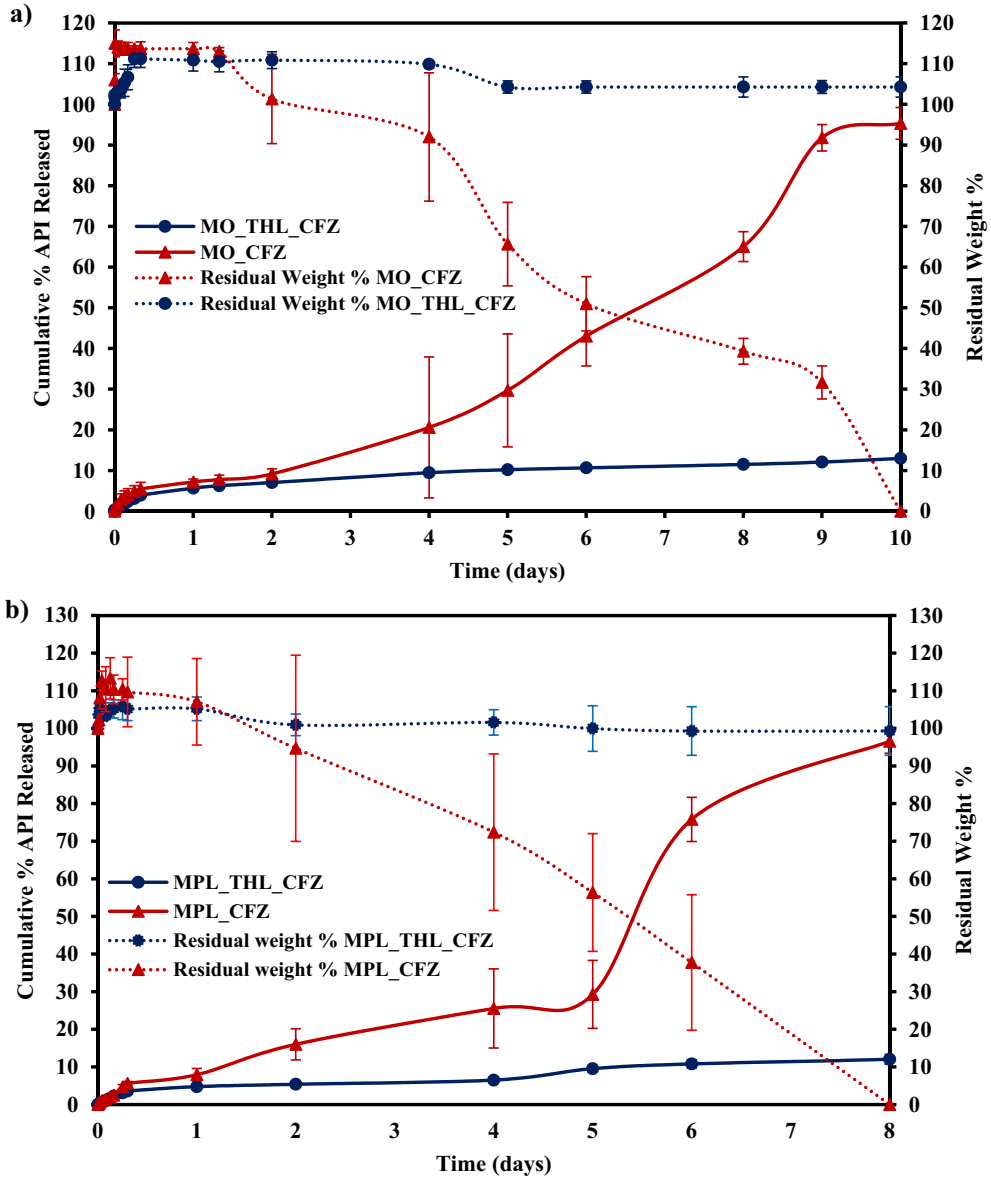


**Fig. 7.** Dissolution profiles of the hydrophobic model drug Clofazimine-citrate salt (1 wt%) from a) MO and b) MPL LCP formulations (Blank or formulated with 1.5% w/w THL) into water incubated at 37 °C in the presence of lipase enzyme showing the corresponding swelling and degradation behavior of the gels. (Water replaced PBS for the release study with CFZ-citrate.) Each point represents a mean value ± standard deviation of three determinations.

As the release kinetics of APIs from LCP depend on their location within the matrix [37], it was expected that the dissolution of the two model agents would follow different kinetics. To highlight the influence of the APIs location within the matrix on its release profile, caffeine was reconstituted in MAG LCP formulations to act as a model hydrophilic agent and the effect of encapsulation with lipase inhibitor THL on its release was studied. Release data was obtained and quantified using HPLC. The dissolution profiles of the hydrophilic model drug from these systems are shown in Fig. 8, plotted with the degradation profiles of the matrices.

It was seen that the MO and MPL LCP systems were comparable as far as the release of the caffeine is concerned, although a slightly slower release was observed from the MO LCP system. The variations in release may once again be attributed to differences in the water channel diameter of the two systems owing to an osmotic effect; whereby different volumes of water can enter the respective network of channels, and is related to the ratio of the molecule size to water channel diameter [10]. It is obvious from the dissolution profiles of these formulations that the release of caffeine was not greatly influenced by the introduction of THL into MAG systems, as simple diffusive mechanisms were driving its release and were largely independent of matrix effect. A decrease in water channel diameter of almost 0.65 nm estimated in the MPL-inhibitor system upon the addition of caffeine may account for the slighter slower elution observed in the inhibitor system [10]. The theories put forward by Clogston and Caffrey suggested that as the size of the water channel approaches the size of the molecule that it encapsulates, the diffusion of said molecule is slowed or prevented. However, the narrower water channel diameter in our systems still well exceeded that of the caffeine molecule, even if it were to exist as a dimer or trimer and so explains the relatively analogous release profiles with and without the THL inhibitor. The SAXS data showed only minor reductions in water channel diameter upon the addition of 1 wt% caffeine to the monoolein LCP-inhibitor system evidenced in the largely comparable release profiles with and without THL. However, the MO-THL samples

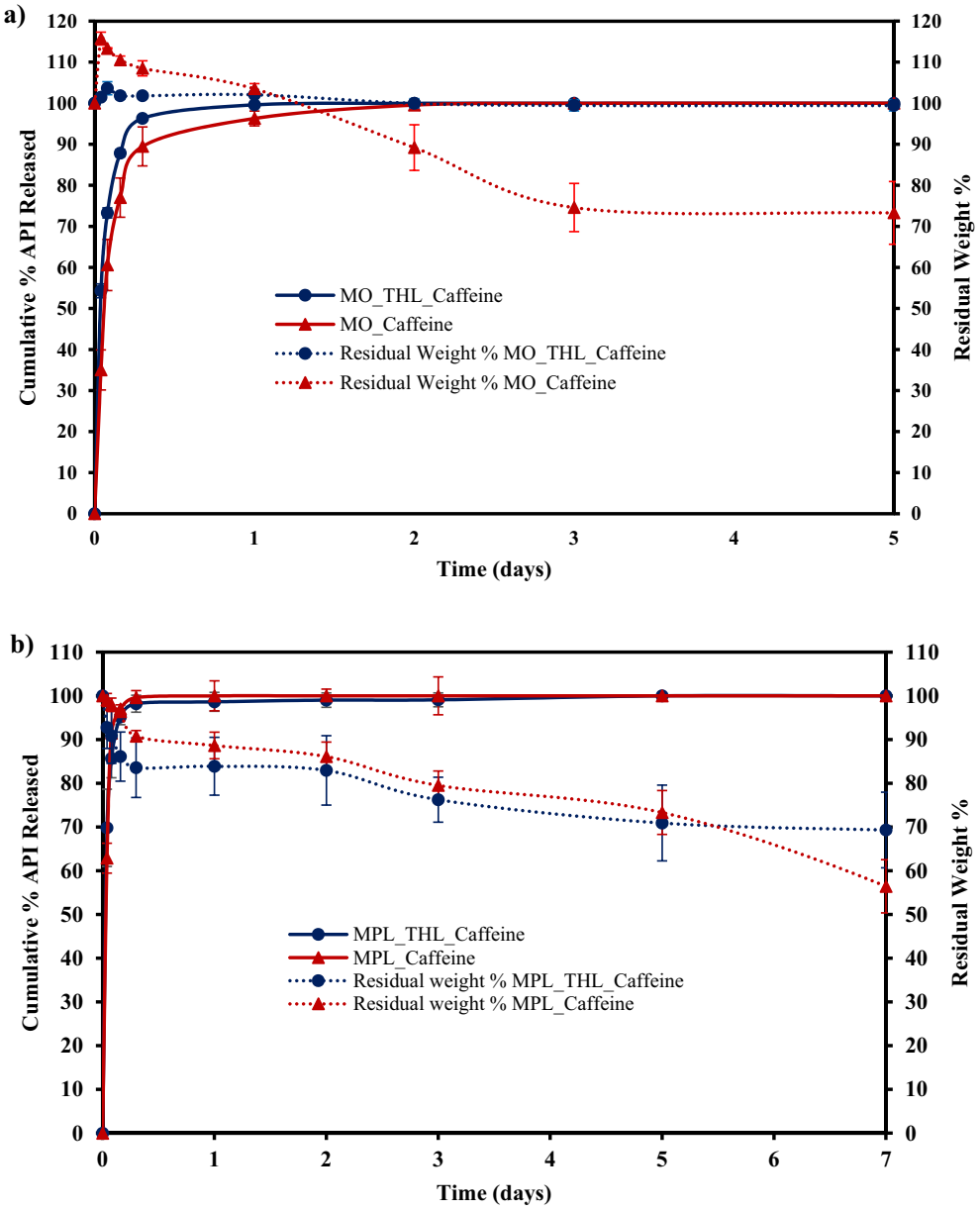


**Fig. 8.** Dissolution profiles of the hydrophilic model drug Caffeine (1 wt%) from a) MO and b) MPL LCP formulations (Blank or formulated with 1.5% w/w THL) into Physiological Buffer (1X PBS pH 7.4) incubated at 37 °C in the presence of Lipase enzyme showing the corresponding swelling and degradation behavior of the gels. Each point represents a mean value ± standard deviation of three determinations.

did display slightly faster diffusive transport compared to the blank MO-caffeine system despite a decrease in water channel diameter of ~0.6 nm, which contradicts the aforementioned theory. It is most likely explained by the fluid nature of the phase as it has been suggested that the inherent flexibility of the liquid crystalline phase may provide evolving fluid channels that facilitate the movement of molecules through the network [10].

The release data collected from the caffeine system was also treated against a number of mathematical models to obtain a correlation coefficient ($r^2$), which allowed for evaluation of the kinetics of release of the hydrophilic model API from LCP. The more simplistic release profile was seen to fit better with the linear models compared to the vastly complex elution behavior seen in the CFZ salt model. The results (supplementary info) indicate that the caffeine does indeed predominantly partition into the aqueous channel network from which it diffuses into the media with little influence from the digestion of the matrix itself. In contrast to the kinetics of CFZ release, when the release data from the various caffeine systems were fitted to the zero-order kinetic equation, the relatively small regression values suggested that the system did not obey the model. However, the dissolution results were found to have a better fit with first order kinetics. The correlation coefficient in this case was closest to unity suggesting that the release of caffeine from LCP most likely follows first order kinetics. This data strongly confirms the expected diffusion-controlled kinetics. In first-order release, the rate of drug diffusion is dependent on the concentration of the API incorporated in the formulation.

Ultimately, this confirms the hypothesis that the incorporation of THL would likely not affect the release kinetics of the hydrophilic agent as its release is, for the most part, independent of the breakdown of the matrix. For this reason, the system would be suitable for a combined therapy application, whereby two or more active agents with opposite solubility properties could be incorporated into the lipid system with the hydrophilic agent being

released within the first few days and more controlled, sustained release of a hydrophobic agent could be achieved.

While this investigation focused primarily on an application with bulk lipid cubic gels, there is recognizable scope to extend this approach further to cubic nanodispersions. In this case, the inhibitor may be encapsulated within the cubosomal network, either pre- or post-fragmentation. The technique of controlling release using inhibitors may be particularly appropriate for these formulations, as cubic nanosystems are more readily degraded by enzymes owing to their increased lipid-media interfacial area. The rate of enzymatic digestion and the length of time required for these nanoparticles to bind with, and be taken up through the cell membrane will influence the release kinetics of an encapsulated drug. Factors such as pH and enzyme concentration in the changing environment of the cubosomes will also influence the release kinetics. One may be interested in tailoring a system depending on the proposed application. For example, a cubosomal-inhibitor hybrid system may be attractive where overcoming the blood–brain barrier is desired, as cubosomes have readily demonstrated their ability to permeate this barrier [95,96]. Here the inhibitor may serve to maintain the nanoparticle architecture for sufficient time to allow successful transition across the barrier to deliver the desired drug at the target site. Future work should focus on exploring these influential factors to distinguish the dominating parameters.

## 4. Conclusions

The development of effective carrier systems that are capable of delivering sustained and therapeutically relevant doses of drugs has earned its place at the forefront of research over the last decade. The amphiphilic, biocompatible, and biodegradable nature of the lipid cubic phase has merited the system as a worthy candidate for controlled delivery. In this study, we have demonstrated that controlled release of hydrophobic APIs can be achieved with a novel formulation approach through the incorporation of small doses of lipase inhibitors, using tetrahydralipstatin as a model. Comprehensive SAXS experiments have shown, notwithstanding some minor alterations in structural parameters, that the incorporation of the inhibitor bore no negative impact on the phase behavior of our lipid cubic formulations below loading concentrations of $\leq$2.5 wt%.

The influence of hydrolytic enzymes on the stability of the cubic phase has been widely demonstrated [35,36,38]. The true effect of these enzymes responsible for catalyzing the hydrolysis of lipid membranes was studied here to better predict the degradation rate of the formulated LCP *in vivo*. Phase stability in the presence of these enzymes was found to control the degradation-driven drug elution. Through the incorporation of THL, the lipid vehicles have demonstrated finely tunable rates of degradation that can be optimally coordinated to release hydrophobic pharmaceutical, and biological molecules over a desired period of time before the gel succumbs to complete digestion. Using CFZ citrate as a model drug, the LCP-inhibitor systems could extend its release profile beyond the one week duration in the blank LCP systems to weeks, and potentially even months through interactions with the lipases responsible for matrix digestion. These hybrid lipid cubic systems may also provide means of delivering inhibitors to control the action of these enzymes. Tetrahydralipstatin is a potent inhibitor of many other lipolytic enzymes additional to the pancreatic lipase studied here. These include gastric lipase, and carboxyl ester lipases. Thus, the approach described here may have a more far-reaching relevance. Should dosage requirements be defined and applied in the formulation, our LCP-inhibitor system could potentially be applied in a variety of drug administration routes with numerous possible target delivery sites where different lipolytic enzymes may be at play. Future work will delve further into the intricacies of the interactions at play between the enzyme inhibitor and the lipid ligand with the hydrolytic enzyme assisted by *in silico* techniques, with an aim of understanding the, what we perceive to be, competitive process. Furthermore, the possibility of applying this technique to cubic dispersions for controlled delivery from the nanosystems will be explored to demonstrate the reach of this approach.

## Funding sources

This work was financially supported by the Irish Research Council under the Enterprise partnership scheme in association with COOK Medical, Ireland.

## CRediT authorship contribution statement

**Michele Dully:** Conceptualization, Methodology, Validation, Formal analysis, Investigation, Writing - original draft, Visualization, Funding acquisition, Data curation. **Christopher Brasnett:** Resources, Writing - review & editing, Visualization, Formal analysis. **Ahmed Djeghader:** Supervision. **Annela Seddon:** Writing - review & editing, Supervision. **John Neilan:** Supervision, Resources. **David Murray:** Supervision, Resources. **James Butler:** Supervision, Resources. **Tewfik Soulimane:** Conceptualization, Resources, Writing - review & editing, Supervision, Project administration, Funding acquisition. **Sarah P. Hudson:** Conceptualization, Resources, Writing - review & editing, Supervision, Project administration, Funding acquisition.

## Declaration of Competing Interest

The authors declare that they have no known competing financial interests or personal relationships that could have appeared to influence the work reported in this paper.

## Acknowledgment

We extend our thanks to Instrument Scientist Nikul Khunti and all staff at Diamond Light Source, Didcot for facilitating the SAXS experiments.

## Appendix A. Supplementary material

Supplementary data to this article can be found online at https://doi.org/10.1016/j.jcis.2020.04.015.

## References

[1] K. Vithani et al., Colloidal aspects of dispersion and digestion of self-dispersing lipid-based formulations for poorly water-soluble drugs, Adv. Drug Deliv. Rev. 142 (2019) 16–34.
[2] M. Gigliobianco et al., Nanocrystals of poorly soluble drugs: Drug bioavailability and physicochemical stability, Pharmaceutics 10 (3) (2018) 134.
[3] J. Barauskas, T. Landh, Phase behavior of the phytantriol/water system, Langmuir 19 (23) (2003) 9562–9565.
[4] J. Clogston, Applications of the lepidic cubic phase: from controlled release and uptake to in meso crystallization of membrane proteins, State University, The Ohio, 2005.
[5] D.J. Hauss, Oral lipid-based formulations: enhancing the bioavailability of poorly water-soluble drugs, CRC Press, 2007.
[6] R. Pandey, G. Khuller, Solid lipid particle-based inhalable sustained drug delivery system against experimental tuberculosis, Tuberculosis 85 (4) (2005) 227–234.
[7] A. Samad, Y. Sultana, M. Aqil, Liposomal drug delivery systems: an update review, Curr. Drug Deliv. 4 (4) (2007) 297–305.
[8] B. Angelov et al., Structural analysis of nanoparticulate carriers for encapsulation of macromolecular drugs, J. Mol. Liq. 235 (2017) 83–89.

[9] A. Angelova, B. Angelov, Dual and multi-drug delivery nanoparticles towards neuronal survival and synaptic repair, Neural Regener. Res. 12 (6) (2017) 886.
[10] J. Clogston, M. Caffrey, Controlling release from the lipidic cubic phase. Amino acids, peptides, proteins and nucleic acids, J. Control. Release 107 (1) (2005) 97–111.
[11] A. S Duttagupta et al., Cubosomes: innovative nanostructures for drug delivery, Current Drug Deliv. 13 (4) (2016) 482–493.
[12] K. Tilekar et al., Cubosomes - a drug delivery system, Int. J. Pharmaceutical, Chem. Biol. Sci. 4 (4) (2014) 812–824.
[13] J.C. Shah, Y. Sadhale, D.M. Chilukuri, Cubic phase gels as drug delivery systems, Adv. Drug Deliv. Rev. 47 (2–3) (2001) 229–250.
[14] P.-O. Eriksson, G. Lindblom, Lipid and water diffusion in bicontinuous cubic phases measured by NMR, Biophys. J . 64 (1) (1993) 129–136.
[15] G. Lindblom, L. Rilfors, Cubic phases and isotropic structures formed by membrane lipids—possible biological relevance, Biochimica et Biophysica Acta (BBA)-Reviews on Biomembranes 988 (2) (1989) 221–256.
[16] E.M. Landau, J.P. Rosenbusch, Lipidic cubic phases: a novel concept for the crystallization of membrane proteins, Proc. Natl. Acad. Sci. 93 (25) (1996) 14532–14535.
[17] V. Luzzati, F. Husson, The structure of the liquid-crystalline phases of lipid-water systems, J. Cell Biol. 12 (2) (1962) 207–219.
[18] H. Qiu, M. Caffrey, The phase diagram of the monoolein/water system: metastability and equilibrium aspects, Biomaterials 21 (3) (2000) 223–234.
[19] R. Forbes, A. Cooper, H. Mitchell, The composition of the adult human body as determined by chemical analysis, J Biol Chem 203 (1) (1953) 359–366.
[20] S. Engström et al., A study of polar lipid drug systems undergoing a thermoreversible lamellar-to-cubic phase transition, Int. J. Pharm. 86 (2–3) (1992) 137–145.
[21] B.J. Boyd, Characterisation of drug release from cubosomes using the pressure ultrafiltration method, Int. J. Pharm. 260 (2) (2003) 239–247.
[22] A. Angelova et al., Proteocubosomes: nanoporous vehicles with tertiary organized fluid interfaces, Langmuir 21 (9) (2005) 4138–4143.
[23] A. Zabara et al., The nanoscience behind the art of in-meso crystallization of membrane proteins, Nanoscale 9 (2) (2017) 754–763.
[24] J. Bender et al., Lipid cubic phases for improved topical drug delivery in photodynamic therapy, J. Control. Release 106 (3) (2005) 350–360.
[25] L. Gan et al., Recent advances in topical ophthalmic drug delivery with lipid-based nanocarriers, Drug Discov. Today 18 (5–6) (2013) 290–297.
[26] D. Wyatt, D. Dorschel, A cubic-phase delivery system composed of glyceryl monooleate and water for sustained release of water-soluble drugs, Pharm. Technol. 16 (10) (1992). 116-116.
[27] C.-M. Chang, R. Bodmeier, Effect of dissolution media and additives on the drug release from cubic phase delivery systems, J. Control. Release 46 (3) (1997) 215–222.
[28] T. Norling et al., Formulation of a drug delivery system based on a mixture of monoglycerides and triglycerides for use in the treatment of periodontal disease, J. Clin. Periodontol. 19 (9) (1992) 687–692.
[29] R. Burrows, J. Collett, D. Attwood, The release of drugs from monoglyceride-water liquid crystalline phases, Int. J. Pharm. 111 (3) (1994) 283–293.
[30] C.M. Chang, R. Bodmeier, Swelling of and drug release from monoglyceride-based drug delivery systems, J. Pharm. Sci. 86 (6) (1997) 747–752.
[31] H. Chung, M. Caffrey, Polymorphism, mesomorphism, and metastability of monoelaidin in excess water, Biophys. J. 69 (5) (1995) 1951–1963.
[32] J. Briggs, The phase behavior of hydrated monoacylglycerols and the design of an X-ray compatible scanning calorimeter, Ths Ohio State University, 1994.
[33] M. Hato et al., Phase behavior of phytanyl-chained akylglycoside/water systems, Trends Colloid Interface Sci. XVI (2004) 56–60.
[34] M. Caffrey, A comprehensive review of the lipid cubic phase or in meso method for crystallizing membrane and soluble proteins and complexes, Acta Crystallographica Section F: Struct. Biol. Commun. 71 (1) (2015) 3–18.
[35] J. Borné, T. Nylander, A. Khan, Effect of lipase on different lipid liquid crystalline phases formed by oleic acid based acylglycerols in aqueous systems, Langmuir 18 (23) (2002) 8972–8981.
[36] R. Wallin, T. Arnebrant, The activity of lipase at the cubic liquid-crystalline phase/water interface, J. Colloid Interface Sci. 164 (1) (1994) 16–20.
[37] S. Fredenberg et al., The mechanisms of drug release in poly (lactic-co-glycolic acid)-based drug delivery systems—a review, Int. J. Pharm. 415 (1–2) (2011) 34–52.
[38] J. Campos et al., On the interaction between adsorbed layers of monoolein and the lipase action on the formed layers, Colloids Surf., B 26 (1–2) (2002) 172–182.
[39] R. Verger, G.H. De Haas, Interfacial enzyme kinetics of lipolysis, Ann. Rev. Biophys. Bioeng. 5 (1) (1976) 77–117.
[40] M.H. Michaelsen et al., The effect of digestion and drug load on halofantrine absorption from self-nanoemulsifying drug delivery system (SNEDDS), AAPS J. 18 (1) (2016) 180–186.
[41] O.M. Feeney et al., 'Stealth'lipid-based formulations: poly (ethylene glycol)-mediated digestion inhibition improves oral bioavailability of a model poorly water soluble drug, J. Control. Release 192 (2014) 219–227.
[42] T. Tran et al., In vitro and in vivo performance of monoacyl phospholipid-based self-emulsifying drug delivery systems, J. Control. Release 255 (2017) 45–53.
[43] Y. Li, D.J. McClements, Inhibition of lipase-catalyzed hydrolysis of emulsified triglyceride oils by low-molecular weight surfactants under simulated gastrointestinal conditions, Eur. J. Pharm. Biopharm. 79 (2) (2011) 423–431.
[44] M. Wulff-Pérez et al., Controlling lipolysis through steric surfactants: new insights on the controlled degradation of submicron emulsions after oral and intravenous administration, Int. J. Pharm. 423 (2) (2012) 161–166.
[45] B.J. Boyd et al., Lyotropic liquid crystalline phases formed from glycerate surfactants as sustained release drug delivery systems, Int. J. Pharm. 309 (1–2) (2006) 218–226.
[46] P. Hadvary, H. Lengsfeld, H. Wolfer, Inhibition of pancreatic lipase in vitro by the covalent inhibitor tetrahydrolipstatin, Biochem. J 256 (2) (1988) 357–361.
[47] Y. Gargouri et al., Inactivation of pancreatic and gastric lipases by THL and C12: 0-TNB: a kinetic study with emulsified tributyrin, Biochimica et Biophysica Acta (BBA)-Lipids Lipid Metabol. 1085 (3) (1991) 322–328.
[48] A.M. Heck, J.A. Yanovski, K.A. Calis, Orlistat, a new lipase inhibitor for the management of obesity, Pharmacotherapy: J. Human Pharmacol. Drug Therapy 20 (3) (2000) 270–279.
[49] M.L. Drent, E.A. van der Veen, First clinical studies with orlistat: a short review, Obes. Res. 3 (S4) (1995) 623S–625S.
[50] M.W. Lee, F.B. Kraemer, D.L. Severson, Characterization of a partially purified diacylglycerol lipase from bovine aorta, Biochimica et Biophysica Acta (BBA)-Lipids Lipid Metabol. 1254 (3) (1995) 311–318.
[51] W. McNeely, P. Benfield, Orlistat, Drugs 56 (2) (1998) 241–249. discussion 250.
[52] F. Winkler, A. d'Arcy, W. Hunziker, Structure of human pancreatic lipase, Nature 343 (6260) (1990) 771.
[53] A. Lookene, N. Skottova, G. Olivecrona, Interactions of lipoprotein lipase with the active-site inhibitor tetrahydrolipstatin (Orlistat) R, Eur. J. Biochem. 222 (2) (1994) 395–403.
[54] D. Lawson, A. Brzozowski, G. Dodson, Lifting the lid off lipases, Curr. Biol 2 (1992) 473–475.
[55] P. Hadvary et al., The lipase inhibitor tetrahydrolipstatin binds covalently to the putative active site serine of pancreatic lipase, J. Biol. Chem. 266 (4) (1991) 2021–2027.
[56] Q. Lüthi-Peng, H.P. Märki, P. Hadváry, Identification of the active-site serine in human pancreatic lipase by chemical modification with tetrahydrolipstatin, FEBS Lett. 299 (1) (1992) 111–115.
[57] B. Borgström, Mode of action of tetrahydrolipstatin: a derivative of the naturally occurring lipase inhibitor lipstatin, Biochimica et Biophysica Acta (BBA)-Lipids Lipid Metabol. 962 (3) (1988) 308–316.
[58] F. Carrière et al., Inhibition of gastrointestinal lipolysis by Orlistat during digestion of test meals in healthy volunteers, Am. J. Physiol.-Gastrointestinal Liver Physiol. 281 (1) (2001) G16–G28.
[59] Human Metabolome Database (HMDB). Orlistat. Available from: http://www.hmdb.ca/metabolites/HMDB0015215.
[60] A. Tiss et al., Transfer of orlistat through oil–water interfaces, Chem. Phys. Lipids 119 (1–2) (2002) 41–49.
[61] A. Tiss et al., Surface behaviour of bile salts and tetrahydrolipstatin at air/water and oil/water interfaces, Chem. Phys. Lipids 111 (1) (2001) 73–85.
[62] P. Bannigan et al., Role of biorelevant dissolution media in the selection of optimal Salt forms of oral drugs: maximizing the gastrointestinal solubility and in vitro activity of the antimicrobial molecule, clofazimine, ACS Omega 2 (12) (2017) 8969–8981.
[63] F. Shakeel, W. Ramadan, Transdermal delivery of anticancer drug caffeine from water-in-oil nanoemulsions, Colloids Surf., B 75 (1) (2010) 356–362.
[64] J. Briggs, H. Chung, M. Caffrey, The temperature-composition phase diagram and mesophase structure characterization of the monoolein/water system, J. Phys. II 6 (5) (1996) 723–751.
[65] J. Filik et al., Processing two-dimensional X-ray diffraction and small-angle scattering data in DAWN 2, J. Appl. Crystallogr. 50 (3) (2017) 959–966.
[66] M. Szlezak et al., Monoolein cubic phase gels and cubosomes doped with magnetic nanoparticles–hybrid materials for controlled drug release, ACS Appl. Mater. Interfaces 9 (3) (2017) 2796–2805.
[67] X.E. Zhou et al., X-ray laser diffraction for structure determination of the rhodopsin-arrestin complex, Sci. Data 3 (2016) 160021.
[68] C.V. Kulkarni et al., Monoolein: a magic lipid?, Phys Chem. Chem. Phys. 13 (8) (2011) 3004–3021.
[69] A. Wade, P. Weller, Lactose, in: Handbook of Pharmaceutical Excipients, 2nd ed., Pharmaceutical Press, London, 1994, pp. 252–261.
[70] D.C. Turner et al., Structural study of the inverted cubic phases of di-dodecyl alkyl-β-D-glucopyranosyl-rac-glycerol, J. Phys. II 2 (11) (1992) 2039–2063.
[71] D.M. Anderson, S.M. Gruner, S. Leibler, Geometrical aspects of the frustration in the cubic phases of lyotropic liquid crystals, Proc. Natl. Acad. Sci. 85 (15) (1988) 5364–5368.
[72] R. Dombrowski, Microscopy techniques for analyzing the phase nature and morphology of biomaterials, in: Characterization of Biomaterials, Elsevier, 2013, pp. 1–33.
[73] E. Lutton, Phase behavior of aqueous systems of monoglycerides, J. Am. Oil Chem. Soc. 42 (12) (1965) 1068–1070.
[74] E. Nazaruk et al., Design and assembly of pH-sensitive lipidic cubic phase matrices for drug release, Langmuir 30 (5) (2014) 1383–1390.
[75] F. Caboi et al., Structural effects, mobility, and redox behavior of vitamin K1 hosted in the monoolein/water liquid crystalline phases, Langmuir 13 (20) (1997) 5476–5483.
[76] C.E. Conn et al., High-throughput analysis of the structural evolution of the monoolein cubic phase in situ under crystallogenesis conditions, Soft Matter 8 (7) (2012) 2310–2321.
[77] B. Tenchov, R. Koynova, G. Rapp, Accelerated formation of cubic phases in phosphatidylethanolamine dispersions, Biophys. J. 75 (2) (1998) 853–866.
[78] V. Cherezov, K.M. Riedl, M. Caffrey, Too hot to handle? Synchrotron X-ray damage of lipid membranes and mesophases, J. Synchrotron Radiation 9 (6) (2002) 333–341.

[79] L. van't Hag et al., Lyotropic liquid crystal engineering moving beyond binary compositional space–ordered nanostructured amphiphile self-assembly materials by design, Chem. Soc. Rev. 46 (10) (2017) 2705–2731.
[80] G.C. Shearman et al., Calculations of and evidence for chain packing stress in inverse lyotropic bicontinuous cubic phases, Langmuir 23 (13) (2007) 7276–7285.
[81] P. Duesing, R. Templer, J. Seddon, Quantifying packing frustration energy in inverse lyotropic mesophases, Langmuir 13 (2) (1997) 351–359.
[82] R. Rand et al., Membrane curvature, lipid segregation, and structural transitions for phospholipids under dual-solvent stress, Biochemistry 29 (1) (1990) 76–87.
[83] R.H. Templer, B.J. Khoo, J.M. Seddon, Gaussian curvature modulus of an amphiphilic monolayer, Langmuir 14 (26) (1998) 7427–7434.
[84] H.G. Edwards et al., Metamorphosis of caffeine hydrate and anhydrous caffeine, J. Chem. Soc., Perkin Trans. 2 (10) (1997) 1985–1990.
[85] J.S. Patton et al., The light microscopy of triglyceride digestion, Food Struct. 4 (1) (1985) 5.
[86] T.G. Kirchgessner et al., Organization of the human lipoprotein lipase gene and evolution of the lipase gene family, Proc. Natl. Acad. Sci. 86 (24) (1989) 9647–9651.
[87] M. Mukherjee, Human digestive and metabolic lipases—a brief review, J. Mol. Catal. B Enzym. 22 (5–6) (2003) 369–376.
[88] D.B. Warren et al., Real time evolution of liquid crystalline nanostructure during the digestion of formulation lipids using synchrotron small-angle X-ray scattering, Langmuir 27 (15) (2011) 9528–9534.
[89] K. Larsson, Cubic lipid-water phases: structures and biomembrane aspects, J. Phys. Chem. 93 (21) (1989) 7304–7314.
[90] M.L. Lynch et al., Enhanced loading of water-soluble actives into bicontinuous cubic phase liquid crystals using cationic surfactants, J. Colloid Interface Sci. 260 (2) (2003) 404–413.
[91] K. Lindell et al., Influence of a charged phospholipid on the release pattern of timolol maleate from cubic liquid crystalline phases, Colloid Sci. Lipids 108 (1998) 111–118.
[92] J. Clogston et al., Controlling release from the lipidic cubic phase by selective alkylation, J. Control. Release 102 (2) (2005) 441–461.
[93] V. Patel, A. Misra, Encapsulation and stability of clofazimine liposomes, J. Microencapsul. 16 (3) (1999) 357–367.
[94] J.R. O'Reilly, O.I. Corrigan, C.M. O'Driscoll, The effect of simple micellar systems on the solubility and intestinal absorption of clofazimine (B663) in the anaesthetised rat, Int. J. Pharm. 105 (2) (1994) 137–146.
[95] H. Azhari et al., Stabilising cubosomes with Tween 80 as a step towards targeting lipid nanocarriers to the blood–brain barrier, Eur. J. Pharm. Biopharm. 104 (2016) 148–155.
[96] H. Azhari, Surface modified cubosomes for drug delivery across the blood-brain barrier, University of Otago, 2018.